



1 **Surface and tropospheric ozone over East Asia and Southeast Asia from**
2 **observations: distributions, trends, and variability**

3 Ke Li^{1,*,#}, Rong Tan^{1,#}, Wenhao Qiao^{1,#}, Taegyung Lee², Yufen Wang¹, Danyuting Zhang¹, Minglong
4 Tang¹, Wenqing Zhao¹, Yixuan Gu¹, Shaojia Fan³, Jinqiang Zhang⁴, Xiaopu Lyu⁵, Likun Xue⁶,
5 Jianming Xu^{7,8}, Zhiqiang Ma^{9,10}, Mohd Talib Latif¹¹, Teerachai Amnuaylojaroen¹², Junsu Gil¹³, Mee-
6 Hye Lee¹³, Juseon Bak¹⁴, Joowan Kim¹⁵, Hong Liao¹, Yugo Kanaya¹⁶, Xiao Lu³, Tatsuya Nagashima¹⁷,
7 Ja-Ho Koo^{2,*}

8 ¹Joint International Research Laboratory of Climate and Environment Change, Jiangsu Key
9 Laboratory of Atmospheric Environment Monitoring and Pollution Control, Collaborative Innovation
10 Center of Atmospheric Environment and Equipment Technology, School of Environmental Science
11 and Engineering, Nanjing University of Information Science and Technology, Nanjing 210044, China

12 ²Department of Atmospheric Sciences, Yonsei University, Seoul 03722, South Korea

13 ³School of Atmospheric Sciences, Sun Yat-sen University, Zhuhai, Guangdong, China

14 ⁴Key Laboratory of Middle Atmosphere and Global Environment Observation, Institute of
15 Atmospheric Physics, Chinese Academy of Sciences, Beijing 100029, China

16 ⁵Department of Geography, Faculty of Social Sciences, Hong Kong Baptist University, Hong Kong,
17 China

18 ⁶Environment Research Institute, Shandong University, Qingdao, China

19 ⁷Shanghai Typhoon Institute, Shanghai Meteorological Service, Shanghai 200030, China

20 ⁸Shanghai Key Laboratory of Meteorology and Health, Shanghai Meteorological Service, Shanghai
21 200030, China

22 ⁹Institute of Urban Meteorology, China Meteorological Administration, Beijing 100089, China

23 ¹⁰Beijing Shangdianzi Regional Atmosphere Watch Station, Beijing 101507, China

24 ¹¹Department of Earth Sciences and Environment, Faculty of Science and Technology, Universiti
25 Kebangsaan Malaysia, Bangi, Selangor, Malaysia

26 ¹²Atmospheric Pollution and Climate Change Research Units, School of Energy and Environment,
27 University of Phayao, Phayao 56000, Thailand

28 ¹³Department of Earth and Environment Sciences, Korea University, Seoul 02841, South Korea

29 ¹⁴Institute of Environmental Studies, Pusan National University, Busan 46241, Republic of Korea

30 ¹⁵Department of Atmospheric Sciences, Kongju National University, Kongju 32588, South Korea

31 ¹⁶Japan Agency for Marine-Earth Science and Technology, Yokohama, Japan

32 ¹⁷National Institute for Environmental Studies, Tsukuba 305-8506, Japan

33 [#]These authors contributed equally

34

35 ^{*}Correspondence to: Ke Li (keli@nuist.edu.cn) and Ja-Ho Koo (zach45@yonsei.ac.kr)



36 **Abstract.** High level of ozone throughout the troposphere is an emerging concern over East Asia and
37 Southeast Asia. Here we analyzed available surface ozone measurements in the past two decades
38 (2005-2021) over eight countries, and ten ozonesonde and aircraft measurements within this region.
39 At surface, seasonal mean ozone over 2017-2021 varies from 30 ppb in Southeast Asia to 75 ppb in
40 summer in North China. The metric of seasonal 95th percentile ozone can identify the multiple hotspots
41 of ozone pollution of over 85 ppb in Southeast Asia. The new WHO peak season ozone standard
42 indicates that both East Asia and Southeast Asia face a widespread risk of long-term exposure. The
43 surface ozone increase in South Korea and Southeast Asia from 2005 was leveling off or even
44 decreased in the past decade, while ozone increase in 2000s over China has amplified after 2013.
45 Surface ozone trends in Japan and Mongolia were flat in the past decade. In the troposphere, the
46 available measurements show an overall increasing tendency at different altitudes from a three-decade
47 perspective and its trend in the past decade remains unclear due to data availability. The difference in
48 tropospheric ozone level between East Asia and Southeast Asia is likely due to the high background
49 ozone from stratospheric intrusion over Northeast Asia. In terms of ozone controls, our results suggest
50 that anthropogenic emissions determine the occurrence of high ozone levels but the underappreciated
51 strong ozone climate penalty, particularly over Southeast Asia, will make ozone controls harder under
52 a warmer climate.

53

54 **1. Introduction**

55 Tropospheric ozone has been a long-lasting threat to public health, crop yield, and climate warming
56 (Chang et al., 2017; DeLang et al., 2021; Lyu et al., 2023). Its importance in dampening carbon sink
57 of forests by reducing productivity is also increasingly recognized in recent years (Cheesman et al.,
58 2024). Tropospheric ozone is mainly produced from the photochemical reactions between nitrogen
59 oxides (NO_x) and volatile organic compounds (VOCs) in the presence of sunlight, and stratosphere-
60 troposphere exchange (STE) can also transport ozone into the troposphere (Neu et al., 2014) and even
61 reach up to the surface under conducive weather conditions (Chen et al. 2024). In particular, high level
62 of tropospheric ozone over East Asia and Southeast Asia is of great concern. The estimated
63 cardiovascular premature mortality attributable to surface ozone is 277,800 (142,900-421,900) in 2019
64 over East Asia and Southeast Asia, accounting for ~50% of its global health burden (Sun et al., 2024).
65 The current surface ozone exposure can reduce the annual crop yield in China, South Korea, and Japan,
66 by ~60, 60, 20 million tonnes for wheat, rice, and maize, respectively (Feng et al., 2022). As such, it



67 is important to elucidate the spatiotemporal distributions of observed ozone from the surface to
68 troposphere over East Asia and Southeast Asia.

69 Surface ozone concentrations have been measured by the nation-level network for more than one
70 decade in many countries. In Japan, surface network since the 1970s revealed a gradual increase in
71 ozone (Nagashima et al. 2017; Kawano et al., 2022) until the past decade where Japanese sites
72 experienced an ozone decrease by -0.8 ± 0.5 ppb yr⁻¹ (Wang et al., 2024). In South Korea, surface ozone
73 has been increasing in the past two decades, leading to the maximum daily 8 h average (MDA8) ozone
74 often exceeding 80 ppb in summer in the Seoul metropolitan area (Kim et al., 2023; Colombi et al.,
75 2023). In China, national surface network was established from 2013 and the widespread rising surface
76 ozone in the past decade positioned China to be one of countries with the highest ozone level
77 worldwide (Lu et al., 2020; Li et al., 2021; Wang et al., 2024). In contrast, Hong Kong, located in
78 China's southern coast, exhibited an overall increase in the surface ozone level by 0.35 ppb yr⁻¹ over
79 1994-2018, but the trend tended to level off in recent years (Wang et al., 2019).

80 In Southeast Asia, surface ozone levels are much smaller than those in East Asia due to the lower
81 anthropogenic emissions and frequent marine air inflow (Ahamad et al., 2020; Sukkhum et al., 2022;
82 Wang et al., 2022a). The previously published analyses on long-term ozone trends in Southeast Asia
83 are scarce, mainly focused on Malaysia and Thailand before 2016. In Malaysia, there was observed
84 ozone increase of 0.09-0.21 ppb yr⁻¹ over the Peninsular Malaysia during 1997-2016 but the Borneo
85 Malaysia recorded small or insignificant ozone trends (Ahamad et al., 2020; Wang et al., 2022a). In
86 Thailand, the observed surface ozone experienced significant increase by 0.7 to 1.2 ppb yr⁻¹ during dry
87 seasons over 2005-2016 (Wang et al., 2022a). In Indonesia, there was no significant ozone trend in
88 Bukit Koto Tabang (a suburban site) over 2005-2016 (Wang et al., 2022a). In Philippines, Salvador et
89 al. (2022) reported an increase of 0.41 ppb yr⁻¹ in surface ozone over 2014-2020 based on air quality
90 measurements in Butuan (an urban site), southern Philippines. Long-term ozone measurements in other
91 Southeast Asia countries were not well documented.

92 Tropospheric ozone profiles and columns over East Asia and Southeast Asia have been measured by
93 multiple platforms including ozonesonde, aircraft, and satellite. By using long-term ozonesonde
94 measurements, previous studies have extensively explored tropospheric ozone profiles in Beijing
95 (Zeng et al., 2023) and Hong Kong (Liao et al., 2020) of China, and in Pohang of South Korea (Bak
96 et al., 2022). However, these ozonesonde-based analyses mainly focused on the spatiotemporal
97 variability and source contributions of tropospheric ozone at the individual site. By using the IAGOS
98 (In-Service Aircraft for a Global Observing System) aircraft ozone observations, Gaudel et al. (2020)
99 show that tropospheric ozone level increases with latitude from Malaysia/Indonesia to Northeast



100 China/South Korea. More importantly, they reported a rapid tropospheric ozone increase in 1994–2016
101 over East Asia and Southeast Asia, consistent with satellite tropospheric ozone column trends
102 (Gopikrishnan and Kuttippurath, 2024), which has been further attributed to the rising anthropogenic
103 emissions both locally and remotely (Wang et al., 2022a; Wang et al., 2022b; Li et al., 2023).
104 Considering that East Asia and Southeast Asia has been identified as a global hot spot with the fastest
105 increase in observed tropospheric ozone after 1990s by the Intergovernmental Panel on Climate
106 Change (IPCC) Sixth Assessment Report (AR6), a comprehensive assessment on tropospheric ozone
107 over this region by using these available measurements is strongly needed.

108 Under the framework of the Tropospheric Ozone Assessment Report (TOAR, 2014-2019), the TOAR
109 documents comprehensively estimate the global ozone pollution and its historical trends. The first-
110 phase TOAR includes only limited ground observation data over East Asia and Southeast Asia
111 countries before 2014 (Chang et al., 2017). In the context of the TOAR Phase Two (TOAR II, 2020-
112 2024), the established East Asia Focus Working Group (EAWG) aims to advance ozone research over
113 East Asia and Southeast Asia, with a focus on observed ozone trends and their attributions. Please see
114 the accompanying paper for ozone trend attributions (Lu et al., 2024). Our effort is to include ozone
115 measurements (or post-calculated ozone metrics) from surface to tropopause collected from TOAR
116 database and individual institutions over East Asia and Southeast Asia.

117 This paper will present the most comprehensive view of ozone distributions and evolution over East
118 Asia and Southeast Asia across different spatiotemporal scales in the past two decades. The structure
119 of this paper is as follows: Section 2 introduces the multiple ozone measurements and calculation of
120 different ozone metrics; Section 3 describes the present-day surface ozone levels with different metrics
121 and long-term surface ozone trends in the past two decades; Section 4 describes the three-dimensional
122 present-day distribution and long-term trends in tropospheric ozone; Section 5 discusses the important
123 implications for future ozone pollution controls; Conclusions are given in Section 6.

124

125 **2. Data and methods**

126 **2.1 Surface ozone observations**

127 In this study, we used surface ozone measurements from national networks of China (2013-2021),
128 Japan (2005-2021), South Korea (2005-2021), Malaysia (2005-2021), and Thailand (2005-2021) that
129 were collected from the TOAR II database or provided by our EAWG members. In addition to the
130 national network records, individual ozone measurement in Ulaanbaatar of Mongolia, Phnom Penh of
131 Cambodia, and Bandung of Indonesia from the Acid Deposition Monitoring Network in East Asia



132 (EANET) was also included. To assess the long-term ozone trend in China before 2013, we also
133 collected 11 ozone measurements from previously-published literatures with updates from our EAWG
134 members. As shown in Table S1, it includes 1 global baseline station (Mt. Waliguan), 4 regional
135 background stations (Akedala, Longfengshan, Xianggelila, and Lin'an), and 1 rural station (Gucheng)
136 from Xu et al. (2020), 1 regional background station (Mt. Tai) from Sun et al. (2016), 1 regional
137 background station (Shangdianzi) from Ma et al. (2016), 1 urban station from Gu et al. (2020), and 1
138 urban station (Guangzhou) and 1 suburban station (Hong Kong) from Zhang et al. (2011).

139 To ensure data quality, the daily and monthly means were calculated using the hourly data when it has
140 over 75% valid data each day and month. To fully assess ozone distributions, we adopted the following
141 ozone metrics in this study: (1) Seasonal mean ozone. Seasonal MDA8 concentrations are calculated
142 for the four seasons (December-January-February, DJF; March-April-May, MAM; June-July-August,
143 JJA; September-October-November, SON), respectively. (2) Ozone exceedance. National ambient
144 ozone air quality standard varies greatly among countries in East Asia and Southeast Asia (Table S2).
145 The threshold for MDA8 ozone ranges from $60 \mu\text{g m}^{-3}$ in Philippines to $160 \mu\text{g m}^{-3}$ in China, and for
146 the maximum daily 1 h average (MDA1) ozone ranges from $120 \mu\text{g m}^{-3}$ in Japan to $235 \mu\text{g m}^{-3}$ in
147 Indonesia. Under standard conditions (1013 hPa, 273 K), $1 \text{ ppb} = 2.14 \mu\text{g m}^{-3}$. In this study, we adopted
148 the thresholds of 60 ppb and 47 ppb (WHO standard) for MDA8 ozone to determine the exceedance
149 days. (3) Peak season ozone. In 2021, the World Health Organization (WHO) newly introduced a
150 standard for the peak season (six-month mean) ozone limit of $60 \mu\text{g m}^{-3}$ to save more people suffering
151 from its long-term exposure. We used this threshold to assessment the peak season ozone levels.

152 **2.2 Tropospheric ozone observations**

153 In this part, we suggest our results from the analysis of vertical ozone profile, mostly based on the
154 ozonesonde measurement and some aircraft measurement. There are a number of ozonesonde
155 measurement sites, but here, we only consider 10 sites (Table S3), which has 10 measurements per
156 year at minimum, and continues at least 5 years for enabling reliable characteristics. Data at 9 sites
157 were obtained from the World Ozone and Ultraviolet Radiation Data Centre (WOUDC), and data at
158 Beijing site was directly provided from Zhang et al. (2021).

159 We also used the altitudinal ozone measurements that have been collected from the In-service Aircraft
160 for a Global Observing System (IAGOS). While the IAGOS mission has been operational since 1990s
161 and still available, ozone data in East Asia are limited. Here we only utilized the IAGOS ozone data
162 from 1995 to 2014, the period having enough number of measurements. Location of all ozonesonde
163 sites and the IAGOS region are shown in Section 4.



164 **2.3 Ozone trend calculation**

165 In terms of ozone distributions, we present the present-day ozone maps averaged over 2017-2021. We
166 required that there are at least three out of these five years of data available in the calculation. In terms
167 of ozone trends: the time frame of 2013-2021 was adopted to represent the past decade trend; the time
168 frame of 2005-2021 was adopted to represent the 21st Century trend and time series should begin at
169 least in the range 2005-2010 and end in the range 2017-2021; the time frame of 1995-2021 was adopted
170 to represent the late 20th century trend and time series should begin at least in the range 1995-1999
171 and end in the range 2017-2021.

172 Following TOAR II guideline, to determine the ozone trend, we first derived the monthly anomalies
173 of ozone concentrations that are calculated as the difference between the individual monthly means
174 and the monthly climatology. Then, a quantile regression method as recommended by TOAR II
175 statistical guidance was employed to estimate the linear trend in surface ozone, and a 50th quantile
176 regression slope was reported in consideration of the length of ozone records.

177

178 **3. Present-day distribution and long-term trends in surface ozone**

179 **3.1 Distribution of present-day surface ozone over 2017-2021**

180 **3.1.1 Seasonal mean MDA8 ozone**

181 Figure 1 shows the seasonal mean MDA8 ozone concentrations averaged over 2017-2021. In winter,
182 seasonal mean ozone level is almost below 50 ppb and it is even decreased to 20-30 ppb in many
183 Chinese cities. The high NO_x emissions in urban environment make ozone strongly titrated and often
184 drop below the Northern Hemisphere background ozone (Vingarzan, 2004). High ozone values of 55-
185 60 ppb in Northern Thailand and 60-65 ppb in Bangkok (Thailand) are notable. In spring, seasonal
186 mean ozone concentrations are doubled in North China (north of 30°N) and increased by 10-20 ppb
187 from wintertime in South Korea and Japan. High ozone of over 60 ppb in Thailand still holds in spring
188 and ozone concentration is enhanced by up to 20 ppb in Yunan province (China), reflecting a possible
189 concentration from spring fire emissions over Southeast Asia (Xue et al., 2021). In summer, the highest
190 ozone levels of over 75 ppb are found in the North China and western China exhibits ozone
191 concentrations of 60-65 ppb. In Southern China, ozone level is decreased to 30~55 ppb because of the
192 active summer monsoon rainfall (Zhou et al., 2022). The hot spot of summer ozone pollution is found
193 in Seoul (South Korea) where seasonal mean ozone is also over 75 ppb, followed by 55~60 ppb in
194 Tokyo (Japan), 40-50 ppb in Kuala Lumpur (Malaysia), 30-40 ppb in Bangkok (Thailand). In autumn,
195 ozone concentrations are decreased strongly from their summer levels in the north of 30°N over East



196 Asia but are increased remarkably in the Pearl River Delta (PRD) region of China where its seasonal
197 mean MDA8 ozone of up to 65 ppb is the highest level within the East Asia and Southeast Asia.

198 In addition to mean ozone level, Figure 2 shows the seasonal 95th percentile ozone concentrations
199 averaged over 2017-2021. The ozone metric is almost the fifth highest value in each season,
200 representing the high ozone values of great concern in air quality management. Although the
201 seasonality of the 95th percentile ozone resembles the mean ozone evolution, the occurrence of the
202 very high 95th percentile ozone values highlights the severity of ozone pollution over East Asia and
203 Southeast Asia. In winter, high ozone of 85-95 ppb occurs over the Southern Thailand, and some cities
204 in PRD region can suffer from ozone level over 75 ppb. In spring, in East Asia the 95th percentile
205 ozone can reach over 95 ppb over Chinese major city clusters and Seoul, and in Southeast Asia ozone
206 level of over 75 ppb occurs in many stations in Thailand and Peninsular Malaysia. In summer, high
207 levels of the 95th percentile ozone appear exclusively over East Asia, with ozone concentrations of
208 over 115 ppb in the North China Plain (NCP), over 105 ppb in the Yangtze River Delta (YRD), and
209 over 95 ppb in PRD, Sichuan Basin, Seoul, and Busan. In addition, some cities (e.g., Tokyo, Osaka) in
210 Japan also have ozone levels over 85 ppb. In autumn, the high ozone levels only concentrate on PRD
211 and YRD regions, with the 95th percentile ozone over 115 ppb in PRD and over 95 ppb in YRD,
212 respectively.

213 3.1.2 Number of days of ozone exceedance

214 Figure 3 shows that the national ozone air quality standard varies greatly in different countries over
215 East Asia and Southeast Asia. For example, MDA8 and MDA1 ozone thresholds in China are 160 $\mu\text{g m}^{-3}$
216 m^{-3} and 200 $\mu\text{g m}^{-3}$, respectively, which lie at the high end of the adopted standards. A lower standard
217 of MDA8 of 140 $\mu\text{g m}^{-3}$ in Thailand and of 120 $\mu\text{g m}^{-3}$ in Vietnam, South Korea, and Singapore are
218 adopted, while Laos, Myanmar, and Philippine adopt a standard consistent with or lower than the WHO
219 guidance. In terms of MDA1 standard, most of the countries adopt a threshold around 200 $\mu\text{g m}^{-3}$. As
220 such, for the sake of health impact assessment, here we adopted the uniform threshold of 60 ppb and
221 WHO guideline to estimate the annual ozone exceedance.

222 Figure 4 shows the annual number of days with MDA8 ozone concentration greater than 60 ppb
223 (NDGT60) and with MDA8 ozone concentration greater than 47 ppb (NDGT47), respectively. In terms
224 of NDGT60, most of the NCP cities in China have ozone exceedance over 125 days, followed by
225 around 100 days in YRD, PRD, and Northwest China. In South Korea, most of the stations experience
226 60-100 days per year with daily MDA8 ozone over 60 ppb, while in Japan it is almost less than 45
227 days except for a few cities. In Southeast Asia, NDGT60 is almost less than 75 days, and particularly



228 Malaysia, Cambodia, and Indonesia have NDGT60 less than 15 days that is consistent with the very
229 low 95th percentile ozone (Figure 2). If the WHO standard is applied, most of the cities in eastern
230 China will have more than 150 days with MDA8 ozone exceedance, and this is also the case for western
231 China. This suggests the pressing challenge to mitigate ozone pollution due to the large-scale high
232 emissions in China. In South Korea, the NDGT47 is over 100 days for most of the stations, which is
233 consistent with the high background ozone issue as reported by Columbi et al. (2023). Ozone
234 exceedance over 100 days for NDGT47 can be also found in major cities in Japan, Thailand, and
235 Malaysia.

236 3.1.3 Peak season ozone levels

237 In this study, we also apply the new WHO standard for peak season ozone to assess risks of long-term
238 ozone exposure over East Asia and Southeast Asia. Figure 5 shows the estimated peak season ozone
239 concentrations averaged over 2017-2021 and its ratio relative to the WHO standard. In China, the NCP
240 region holds the highest peak season ozone of over 70 ppb that is about 2.5 times the WHO threshold,
241 followed by 65 ppb in YRD, 55 ppb in PRD, SCB, and some cities of Northwest China. More
242 importantly, the lowest peak season ozone in China is still higher than the WHO standard, suggesting
243 the difficulty in mitigation long-term ozone exposure over China. In South Korea, the peak season
244 ozone is well above 55 ppb and even higher than 60 ppb, again reflecting the important role of
245 background ozone in South Korea. In Japan, the peak season is mainly within the range from 40 to 55
246 ppb, amounting to 1.5-2 times the WHO standard. In Ulaanbaatar of Mongolia, the peak season ozone
247 is below 20 ppb. In Southeast Asia, Thailand has the highest peak season ozone of over 60 ppb around
248 Bangkok, and high values of 55-60 ppb are also found in the northern Thailand and southern coastal
249 Thailand. In Malaysia, the Peninsular Malaysia has peak season ozone of 30-50 ppb, higher than the
250 WHO standard. However, the Borneo Malaysia, Cambodia, and Indonesia record peak season ozone
251 lower than the WHO standard. Overall, the estimated peak season ozone level shows that 98% stations
252 in East Asia and Southeast Asia are above the WHO standard, and suggests the urgent need to reduce
253 long-term ozone exposure risks.

254 3.2 Surface ozone trends in the past two decades

255 3.2.1 2005-2021 ozone trends

256 Figure 6 shows the observed ozone trends in different seasons over the period of 2005-2021. Due to
257 the availability of long-term surface measurements, we only present ozone trends over South Korea,
258 Japan, Thailand, and Malaysia. In South Korea, increasing ozone trends with high certainty are notable
259 across different seasons ranging from 0.48 ppb yr⁻¹ in winter to 0.96 ppb yr⁻¹ in summer. In Japan,



260 observed ozone shows a decreasing tendency from 2005 to 2021 in summer but an extensive ozone
261 increase by 0.28 ppb yr^{-1} in wintertime. In Thailand, there is an overall increasing trend in surface
262 ozone but with spatial heterogeneity over 2005-2021. Specifically, significant ozone increase mainly
263 occurs over northern Thailand and southern coastal Thailand, while ozone increase around Bangkok
264 is much smaller or insignificant. In Malaysia, there is a wintertime ozone increase by 0.2 ppb yr^{-1}
265 particularly in three sites in Peninsular Malaysia and in five sites in Borneo Malaysia, while in other
266 seasons the observed ozone trends over 2005-2021 are small and statistically insignificant. The
267 estimated increasing tendency in surface ozone since 2005 is in agreement with Kim et al (2023) for
268 2001-2021 ozone increase in South Korea and with Wang et al. (2022) for 2005-2016 ozone increase
269 in Southeast Asia.

270 Due to the lack of national network measurement before 2013 in China, we also compiled 11 individual
271 ozone measurements (8 background/rural sites and 3 urban sites) that are available from around 2005
272 (see Data and methods). Figure 7 and Table S1 show the estimated seasonal ozone trends in these 11
273 stations by using the metrics of MDA8 ozone and 24-hour mean ozone. The Mt. Waliguan, a global
274 baseline station of the World Meteorological Organization /Global Atmosphere Watch (Xu et al., 2020),
275 shows statistically significant ozone increase by 0.56 ppb yr^{-1} in spring. However, at the multiple
276 regional background stations located in western boundary of China (Xianggelila, Akedala) and eastern
277 boundary of China (Lin'an, Longfengshan), there is no such a consistent ozone increase but with large
278 variability across different seasons, suggesting the important role of regional emission change and
279 climate variability (Zhang et al. 2023, Ye et al., 2024). In the NCP, one of the regions with the highest
280 present-day ozone level, the observed ozone after 2005 at the regional background sites (Shangdianzi,
281 Mt. Tai) and rural site (Gucheng) experienced a consistently increasing trend in spring and summer
282 seasons. In Shangdianzi, the MDA8 ozone trend over 2005-2019 is 0.85 ppb yr^{-1} ($p < 0.1$) in spring and
283 0.73 ppb yr^{-1} ($p = 0.12$) in summer, respectively. The similar seasonal trends are also shown in Gucheng
284 (a rural site close to Shangdianzi) and Mt. Tai (located in the center of NCP). It is noted that summer
285 ozone trends in Mt. Tai over 2005-2019 also have strong intraseasonal variability, with much faster
286 ozone increase in July and August (Sun et al., 2016). In addition to the background/rural sites, urban
287 sites in YRD (Xujiahui) and PRD (Guangzhou, Hong Kong) record the urban ozone increase after
288 2005 that has been attributed to anthropogenic emissions and circulation patterns in previous studies
289 (Wang et al., 2019; Gu et al., 2020; Cao et al., 2024).

290 **3.2.2 2013-2021 ozone trends**

291 Figure 8 shows the observed ozone trends in different seasons over the period of 2013-2021. Here we
292 include ozone trends over China, Mongolia, Japan, South Korea, Malaysia, and Thailand. In China,



293 there is a widespread ozone increase throughout the year, with mean ozone increase of 1.0-1.2 ppb yr⁻¹
294 ¹ in different seasons, which is only half of the ozone increase over 2013-2019 in China (Lu et al.,
295 2020; Li et al., 2020). Spatially, ozone increase mainly occurs in the northern China and western China.
296 Seasonally, there is fast ozone increase in winter over the NCP region, suggesting the urgency of
297 wintertime ozone regulation (Li et al., 2021). In South Korea, the 2005-2021 ozone rise is strongly
298 mitigated over 2013-2021 when summer ozone trend is only 0.45 ppb yr⁻¹. In Mongolia, there is a
299 notable spring ozone increase but with low certainty. In Southeast Asia, however, the observed ozone
300 in Malaysia and Thailand shows a decreasing tendency in most of the sites, which is contrary to the
301 over ozone increase from 2005 to 2021. Overall, except for the rapid ozone increase over China in the
302 past decade, there is a leveling off or decrease in surface ozone trend over other countries in the
303 meantime.

304 To further examine the long-term ozone variability, we also show the time series of observed national
305 MDA8 ozone concentrations during warm seasons from 2005 to 2021 in Figure 9. In South Korea,
306 there is a flat trend in ozone over 2017-2021 after a sustained ozone increase since 2015, and there is
307 no clear trend in warm-season ozone in Japan due to the limited data availability. In Southeast Asia,
308 after 2013, surface ozone in Malaysia starts to decline and ozone trend in Thailand levels off. This is
309 also demonstrated in the warm-season ozone trend in Figure S1. In addition, we also find the large
310 interannual variability in observed ozone concentration that deserves further investigation. For
311 example, in 2017, there is strong surface ozone enhancement relative to 2016 in China, Japan, and
312 South Korea, while surface ozone is consistently decreased in Mongolia, Thailand, and Malaysia.
313 Previous studies have linked the changes in large-scale circulations to this extensive ozone anomalies
314 (e.g., Yin et al., 2010; Jiang et al., 2021).

315

316 **4. Present-day distribution and long-term trends in tropospheric ozone**

317 **4.1 Three-dimensional distribution of present-day tropospheric ozone**

318 First, we compared climatological mean vertical ozone profile (from surface to 10 km altitude) using
319 the ozonesonde data (Figure 10). Beijing site in China shows the highest, but Sepang Jaya site in
320 Malaysia shows the lowest ozone mixing ratio through the troposphere. In general, ozone mixing ratio
321 in East Asia (Beijing in China, Pohang in Korea, and Tsukuba in Japan) is higher than that in Southeast
322 Asia (Sepang Jaya in Malaysia and Watukosek in Indonesia). This pattern is well found when we
323 compared average ozone mixing ratio at 1, 3, 5, and 7 km altitude (Figure 11). While some sites show



324 the higher ozone mixing ratio in the boundary layer (e.g., Watukosek), but generally free tropospheric
325 (above 1-2 km height) ozone mixing ratio is higher. Especially, Beijing, Pohang, Sapporo, and Tsukuba
326 sites show large enhancement of ozone above 8 km altitude (Figure 11a), implying that the
327 stratospheric ozone is used to be strongly intruded into the troposphere. Actually ozone mixing ratio
328 values in these 4 sites are highest at 3, 5, and 7 km altitudes, indicating the effect of stratospheric ozone
329 to the enhancement of tropospheric ozone. These 4 sites are located over the Korean peninsula (Figure
330 10) where sudden increase of ozone usually occurs below the tropopause (Park et al., 2012).

331 Seasonal pattern of vertical ozone profile was continually investigated (Figure 12). Tropospheric ozone
332 values at Beijing, Pohang, Sapporo, and Tsukuba site where strong stratospheric ozone intrusion occurs,
333 are generally high in spring (MAM) and summer (JJA). This pattern can be explained by the frequent
334 intrusion of stratospheric ozone in spring (Park et al., 2012), and strong photochemical ozone
335 production that is typical characteristic in summer. In several sites (e.g., Beijing and Tsukuba),
336 photochemical ozone production in summer makes the boundary layer ozone much higher than free-
337 tropospheric ozone. Stratospheric ozone intrusion in these 4 sites is also strong in winter, but does not
338 result in high tropospheric ozone due to weak photochemistry in winter. Ozone values at Kagoshima
339 (Japan), Naha (Japan), King's park (Hongkong), and Hanoi (Vietnam) that are located below 30 °N,
340 however, are lowest in the lower troposphere. Considering that these sites are easily affected by the
341 inflow of maritime air mass under the trade-wind influence, this low summertime ozone can be
342 explained by the transport of humid and ozone-poor air mass from the ocean due to the monsoon
343 system (Zhao and Wang, 2018; Jiang et al., 2021). Sites in equatorial region (i.e., Sepang Jaya and
344 Watukosek) do not have large seasonal variation of tropospheric ozone.

345 We repeated same analysis using the IAGOS data (Figure 13). IAGOS ozone profiles over Northeast
346 Asia also reveal the highest tropospheric ozone in summer (June), and lowest in winter (December).
347 We can also see large enhancement of summertime ozone in the boundary layer associated with strong
348 photochemistry, and highest ozone in winter (DJF) and spring (MAM) above 8 km altitude, implying
349 the intrusion of stratospheric ozone. Monthly variation of ozone at multiple heights (Figure 13b)
350 illustrates a sharp drop of ozone from June to July, depicting the wash-out effect due to the rainy season
351 called Jangma (Korea) or Maiyu (China). Overall, ozone profile pattern in Northeast Asia from the
352 long-term aircraft monitoring is similar to findings based on ozonesonde measurements. Among them,



353 we would highlight that the site showing high tropospheric ozone (e.g., Beijing in China, Pohang in
354 Korea, Sapporo in Japan), which are located in Northeast Asia and latitude is higher than 35 °N (Table
355 S3), relate to the strong intrusion of stratospheric ozone. Considering recent studies addressing that
356 background ozone in Northeast Asia is unexpectedly high (Lee and Park, 2022; Columbi et al., 2023),
357 we need to put more weight on the study about the contribution of stratospheric air masses to the
358 Northeast Asian background ozone. Also, some previous studies reported cases of the tropospheric
359 ozone enhancement in Southern China affected by the influence of typhoon (Zhan and Xie, 2022; Li,
360 F. et al., 2023), which are typically explained based on the stratospheric ozone intrusion driven by the
361 deep convection (Chen et al., 2022). While those reported cases look significant, however, our results
362 in sites typically affected by typhoon (e.g., Naha, King's park) reveal that it may not contribute to
363 significant increase of summertime mean tropospheric ozone. We also added analyzed results using
364 the IAGOS measurements in Southeast Asia, but the measurements were performed in some limited
365 periods. There is no available data after 2012, and the number of data is enough to analyze only for the
366 year 1995, 1996, 1997, 1999, and 2005. Thus, we did not deeply interpret IAGOS results in Southeast
367 Asia, but simply reported themselves.

368 **4.2. Altitudinal long-term trends of tropospheric ozone**

369 In addition to the spatial distribution of tropospheric ozone, we investigate the long-term trend of ozone
370 mixing ratio in a vertical scale using the ozonesonde measurements. We confirmed the time-series
371 analysis at each altitude (Figure S2) and performed the Mann-Kendall test. Finally, we estimated long-
372 term ozone trend in the troposphere (from surface to 10 km altitude) per 100 m interval vertically with
373 the information of statistical significance. These results are shown in Figure 14.

374 At first, we can see increasing trend of tropospheric ozone in some East Asian sites that we are treating.
375 Increasing trend of ozone mixing ratio about 1-2% per year is found at Sapporo, Naha, and Hanoi
376 consistently through whole troposphere (Figure 14a, 14e, and 14g). Tsukuba and Pohang sites have
377 similar pattern but smaller trend (~0.5-1 % per year). Ozone in King's park, Sepang Jaya, and
378 Watukosek are only increasing in the boundary layer (below ~2-3 km), but almost no significant long-
379 term trend in the free troposphere. Kagoshima and Beijing sites are totally opposite; There are
380 decreasing trends through whole troposphere. In brief, we can classify 3 types of long-term trends of
381 tropospheric ozone in East Asia: (1) Increase through whole troposphere, (2) Increase only in the



382 boundary layer and no clear trend in the free troposphere, and (3) Decrease through whole troposphere.

383 We also examined trends using the seasonal mean ozone mixing ratio: MAM in Figure S3, JJA in
384 Figure S4, SON in Figure S5, and DJF in Figure S6. Overall, we can split two different patterns such
385 as seasonally consistent and inconsistent trends. Tropospheric ozone at Sapporo, Tsukuba, and Naha
386 has been consistently increasing trends in all seasons. In contrast, Tropospheric ozone at Beijing
387 reveals consistent decreasing trend, only with some exception. Some exceptions are increasing trends
388 near the surface in DJF and MAM. While these are not statistically significant, it seems required to put
389 our eyes here more because near-surface ozone increase in high polluted area directly connects to the
390 human health and crop damage. We can state that tropospheric ozone trend at King's park (increasing),
391 Hanoi (increasing), and Kagoshima (decreasing) is rather consistent in all seasons, but the extent of
392 trend varies largely according to the season. Trends at Pohang, Sepang Jaya, Watukosek are seasonally
393 different. Ozone trends at Pohang are clearly positive in JJA and SON but almost none or even partly
394 negative in upper heights in DJF and MAM Trends at Sepang Jaya are only positive in DJF, but
395 generally none or negative in other seasons. Ozone at Watukosek shows the distinguished increasing
396 only in MAM. These features imply that a certain season has matchless trend value and it can lead
397 whole trend pattern in that site.

398 We finally estimated the long-term trend of tropospheric ozone in East Asia using the IAGOS aircraft
399 measurements (Figure S7). Data is only available from 1995 to 2014, therefore recent decade situation
400 (e.g., the outbreak of Coronavirus disease 2019) is not included here. In spite of this limitation,
401 generally we can see the increasing trend of tropospheric ozone in East Asia, consistent with previous
402 reports (Wang et al., 2019; Lee et al., 2021; Li, S. et al., 2023). Seasonally, however, trends are rather
403 different; There are clear increasing trends during JJA and SON, but almost no trend with partial
404 decreasing trend in the upper troposphere during DJF and MAM. Partial decreasing trends in DJF and
405 MAM look similar to a recent report addressing that stratospheric ozone transport to the troposphere
406 in has been weakened (Chen et al., 2024), but overall, tropospheric ozone in East Asia reveals large
407 increasing trends in warm season (JJA and SON), and it seems to lead to an overall ozone increase in
408 East Asia.

409



410 **5. Implications for ozone control**

411 Our research reveals significant spatial and seasonal ozone variations over East Asia and Southeast
412 Asia. Spatially, ozone levels are closely associated with anthropogenic emissions (e.g., NO_x emissions),
413 with high ozone concentrations aligning well with NO_x emission patterns observed through ground-
414 based and satellite measurements. Figure 15 shows the bottom-up NO_x emissions and the satellite-
415 derived NO₂ columns over East Asia and Southeast Asia. Seasonally, ozone variations are primarily
416 influenced by meteorological conditions and biomass burning emissions in Southeast Asia. For
417 example, ozone peaks usually occur in northern China during summer, in the Pearl River Delta during
418 autumn, and in Southeast Asia during spring.

419 Relative to East Asia, although the health risks in Southeast Asia are relatively low under short-term
420 ozone exposure indicators (e.g., 95th percentile ozone concentration), the WHO newly introduced peak
421 season ozone concentration standard indicates that both East Asia and Southeast Asia are faced with a
422 widespread risk of long-term ozone exposure, with the vast majority of the region exceeding WHO
423 standards. In addition to health impacts, the pervasive ozone pollution in East Asia and Southeast Asia
424 is also threatening global food security by its accounting for over 60% of global rice yield (Feng et al.
425 2022; Yuan et al., 2022). For example, the year-around mean MDA8 ozone over 40 ppb over Southeast
426 Asia suggests the high ozone exposure over a threshold of 40 ppb (AOT40) that is commonly used to
427 investigate ozone effects on vegetation yield (Feng et al. 2022).

428 In addition to the well-known fast-changing anthropogenic emissions over East Asia (Zheng et al.,
429 2018) and Southeast Asia (Wang et al., 2022), our study shows that there is a very strong ozone climate
430 penalty over East Asia and Southeast Asia. Figure 16 shows the observed 50th percentile regression
431 slope between MDA8 ozone and temperature in different seasons averaged over 2017-2021. In East
432 Asia, the locations of high ozone-temperature slope of 3-5 ppb °C⁻¹ in different seasons are consistent
433 with the observed high level of surface ozone. The highest slope of over 5-8 ppb °C⁻¹ is found over the
434 PRD and Sichuan Basin in summer. In Southeast Asia, however, we find a widespread high ozone-
435 temperature slope. In Thailand, the ozone-temperature slope of over 3 ppb °C⁻¹ can be found
436 throughout the year expect for summer. In Malaysia, a strong slope of 4-8 ppb °C⁻¹ persists all the year
437 around that is consistent with a ten-year analysis in Kuala Lumpur by Ashfold et al. (2024). More
438 importantly, the observed 95th percentile regression shows a notably increased ozone-temperature
439 slope over Southeast Asia (Figure S8), suggesting a stronger ozone climate penalty under extreme
440 conditions. In contrast, the IPCC AR6 only identified East Asia and India as the hotspot of ozone
441 climate penalty (Zanis et al., 2022). Our observed-based results highlight the strongly underestimated
442 ozone climate penalty over Southeast Asia.



443 The long-term trend of surface ozone indicates that, based on the available data, high-emission regions
444 in South Korea, Southeast Asia, and China have generally experienced an increase in ozone levels
445 since 2005. However, since 2013, the increase in ozone levels in China has significantly accelerated,
446 while the ozone trends in Thailand and Malaysia in Southeast Asia show no significant changes.
447 Therefore, it is still urgent to attribute the varying ozone trends in East Asia and Southeast Asia across
448 different seasons over the past decade.

449 In the troposphere, the available ozonesonde and IAGOS measurements not only demonstrate the high
450 background ozone in warm seasons over Northeast Asia, but also show an overall increasing tendency
451 in the past three decades. While the increase in tropospheric ozone can be largely attributed to the
452 increased anthropogenic emissions as demonstrated in our companion paper (Lu et al., 2024), the
453 origin of high seasonal background ozone in Northeast Asia remains unclear. Recent studies provide
454 some observational and modeling evidence of stratospheric intrusion (Chen et al., 2024; Columbi et
455 al., 2023) to explain this high background ozone, but a quantitative assessment is urgently needed. In
456 particular, the recent ASIA-AQ campaign (<https://espo.nasa.gov/asia-aq>) flying across Asia countries
457 would be important to understand the high tropospheric ozone issue over East Asia and Southeast Asia.

458

459 **6. Conclusions**

460 Under the framework of the TOAR II (2020-2024) that aims to estimate global and regional
461 tropospheric ozone pollution and its historical trend, in this study we present the most comprehensive
462 view of ozone distributions and evolution over East Asia and Southeast Asia across different
463 spatiotemporal scales in the past two decades. This is done by taking advantage of the available surface
464 ozone measurement in the past two decades (2005-2021) over eight countries, and ten ozonesonde and
465 in-service aircraft measurements within this region. The key conclusions are as follows:

466 Firstly, there are significant spatial and seasonal ozone variations at the present-day level. In summer,
467 seasonal mean MDA8 ozone averaged over 2017-2021 varies from 30 ppb in Southeast Asia to over
468 75 ppb in summer in North China and Seoul. Southeast Asia in winter and spring has high mean ozone
469 of 60 ppb in Thailand. The seasonality of the 95th percentile ozone resembles the mean ozone evolution,
470 but the widespread occurrence of the very high 95th percentile ozone of over 85 ppb highlights the
471 severity of ozone pollution. If the WHO standard is applied for short-term exposure, a large fraction
472 the sites will have more than 100 days with MDA8 ozone exceedance. In terms of long-term exposure,
473 the WHO newly-introduced peak season ozone standard indicates that both East Asia and Southeast



474 Asia are faced with a widespread risk of long-term ozone exposure.

475 Secondly, the surface ozone increase in the past two decades is widespread. In particular, South Korea
476 has a national ozone increase with high certainty across different seasons. In Thailand, there is an
477 overall increasing trend in surface ozone but with spatial heterogeneity over 2005-2021. In China, the
478 compiled 11 individual measurements show an overall ozone increase in high-emission regions and at
479 a global baseline station. However, the observed national surface ozone increase in South Korea and
480 Southeast Asia from 2005 is leveling off or even decreased in the past decade (2013-2021), while
481 ozone increase in 2000s over China has amplified after 2013. Surface ozone trends in Japan and
482 Mongolia are generally flat in the past decade.

483 Thirdly, in the troposphere, the high ozone levels in spring and summer at Beijing, Pohang, Sapporo,
484 and Tsukuba site are driven by strong photochemical ozone production and stratospheric ozone
485 intrusion, supported by both the ozonesonde and IAGOS measurements. The difference in tropospheric
486 ozone level between East Asia and Southeast Asia is likely due to the high background ozone from
487 stratospheric intrusion over Northeast Asia. In terms of ozone trends, from a three-decade perspective,
488 the available ozonesonde and aircraft measurements show an overall increasing tendency at different
489 altitudes but feature with strong site-by-site differences. Due to measurement availability, ozone trend
490 in the past decade is still unquantified.

491 Fourthly, the significant spatial ozone variations over East Asia and Southeast Asia are closely
492 associated with anthropogenic emissions, supported by ground-based and satellite measurements. Our
493 study also shows that there is a very high ozone climate penalty over East Asia and Southeast Asia,
494 and the widespread high ozone-temperature slope of 3-8 ppb °C⁻¹ persists all the year around in
495 Southeast Asia. More importantly, the observed 95th percentile regression shows a notably increased
496 ozone-temperature slope over Southeast Asia, suggesting a critical issue in future ozone controls.

497

498

499

500



501 **Data availability.** All data used in this study, including the observations, meteorological reanalysis
502 and emission data will be archived in a freely-accessed data portal upon the publication of the
503 manuscript.

504 **Supplement.** The supplement related to this article is available online.

505 **Author contributions.** K.L. and J.H.K. led and organized the project, working as the co-leads of the
506 East Asia Working Group of Tropospheric Ozone Assessment Report Phase II (TOAR II) with X.L.
507 and T.N. S.J.F., J.Q.Z., X.P.L., L.K.X., J.M.X., Y.X.G., Z.Q.M., M.T.L., T.A., J.G., M.H.L., J.B., J.K.,
508 J.H.K., X.L., and T.N. assisted in preparation of observational data. K.L., R.T., W.H.Q., and J.H.K.
509 conducted the analysis and prepared the figures. T.L., Y.F.W., D.Y.T.Z., M.L.T., W.Q.Z. contributed to
510 preparing the figures. K.L. and J.H.K. wrote the draft with inputs from H.L. All authors contributed to
511 improving the manuscript.

512 **Competing interests.** Some authors are members of the editorial board of Atmospheric Chemistry and
513 Physics.

514 **Acknowledgements.** We greatly thank the China's Ministry of Ecology and Environment, Korean
515 Ministry of Environment, National Institute for Environmental Studies, Malaysia Department of
516 Environment, Thailand Pollution Control Department, the Acid Deposition Monitoring Network in
517 East Asia (EANET), World Ozone and Ultraviolet Radiation Data Centre (WOUDC), and In-service
518 Aircraft for a Global Observing System (IAGOS) for running the ozone observation networks. We also
519 thank the previous and current TOAR Steering Committee members (Owen Cooper, Lin Zhang, and
520 Keding Lu) for effortless support of guiding the East Asia Working Group of Tropospheric Ozone
521 Assessment Report Phase II (TOAR II).

522

523 **Financial support.** This research was supported by the National Natural Science Foundation of China
524 (grants 42293323, 42205114, and 42293321), the Natural Science Foundation of Jiangsu Province
525 (BK20240035). This work was also supported by the National Research Foundation of Korea (NRF)
526 grant funded by the Korea government (MSIT) (RS-2023-00219830).

527

528

529

530



531 **Reference**

- 532 Ahamad, F., Griffiths, P. T., Latif, M. T., Juneng, L., and Xiang, C. J.: Ozone Trends from Two Decades
533 of Ground Level Observation in Malaysia, *Atmosphere*, 11, 10.3390/atmos11070755, 2020.
- 534 Ashfold, M. J., Latif, M. T., Mokhtar, A. M., Samah, A. A., Mead, M. I., and Harris, N.: The
535 Relationship between Ozone and Temperature in Greater Kuala Lumpur, Malaysia. *Aerosol Air*
536 *Qual. Res.*, 24, 240072, 2024.
- 537 Bak, J., Song, E. J., Lee, H. J., Liu, X., Koo, J. H., Kim, J., Jeon, W., Kim, J. H., and Kim, C. H.:
538 Temporal variability of tropospheric ozone and ozone profiles in the Korean Peninsula during the
539 East Asian summer monsoon: insights from multiple measurements and reanalysis datasets, *Atmos.*
540 *Chem. Phys.*, 22, 14177-14187, 10.5194/acp-22-14177-2022, 2022.
- 541 Cao, T. H., Wang, H. C., Li, L., Lu, X., Liu, Y. M., and Fan, S. J.: Fast spreading of surface ozone in
542 both temporal and spatial scale in Pearl River Delta, *J. Environ. Sci.*, 137, 540-552,
543 10.1016/j.jes.2023.02.025, 2024.
- 544 Chang, K. L., Petropavlovskikh, I., Cooper, O. R., Schultz, M. G., and Wang, T.: Regional trend
545 analysis of surface ozone observations from monitoring networks in eastern North America,
546 Europe and East Asia, *Elementa*, 5, 10.1525/elementa.243, 2017.
- 547 Cheesman, A. W., Brown, F., Artaxo, P., Farha, M. N., Folberth, G. A., Hayes, F. J., Heinrich, V. H. A.,
548 Hill, T. C., Mercado, L. M., Oliver, R. J., O' Sullivan, M., Uddling, J., Cernusak, L. A., and Sitch,
549 S.: Reduced productivity and carbon drawdown of tropical forests from ground-level ozone
550 exposure, *Nat. Geosci.* 17, 10.1038/s41561-024-01530-1, 2024.
- 551 Chen, Z. X., Liu, J. N., Qie, X. S., Cheng, X. G., Yang, M. M., Shu, L., and Zang, Z.: Stratospheric
552 influence on surface ozone pollution in China, *Nat. Commun.*, 15, 10.1038/s41467-024-48406-x,
553 2024.
- 554 Chen, Z. X., Liu, J. N., Qie, X. S., Cheng, X. G., Shen, Y. K., Yang, M. M., Jiang, R. B., and Liu, X.
555 K.: Transport of substantial stratospheric ozone to the surface by a dying typhoon and shallow
556 convection, *Atmos. Chem. Phys.*, 22, 8221-8240, 10.5194/acp-22-8221-2022, 2022.
- 557 Colombi, N. K., Jacob, D. J., Yang, L. H., Zhai, S., Shah, V., Grange, S. K., Yantosca, R. M., Kim, S.,
558 and Liao, H.: Why is ozone in South Korea and the Seoul metropolitan area so high and increasing?,
559 *Atmos. Chem. Phys.*, 23, 4031-4044, 10.5194/acp-23-4031-2023, 2023.
- 560 DeLang, M.N., Becker, J.S., Chang, K.L., Serre, M.L., Cooper, O.R., Schultz, M.G., Schröder, S., Lu,
561 X., Zhang, L., Deushi, M. and Josse, B.: Mapping yearly fine resolution global surface ozone
562 through the Bayesian maximum entropy data fusion of observations and model output for 1990–
563 2017. *Environ. Sci. Tech.*, 55(8), 4389-4398, 2021.
- 564 Feng, Z. Z., Xu, Y. S., Kobayashi, K., Dai, L. L., Zhang, T. Y., Agathokleous, E., Calatayud, V., Paoletti,
565 E., Mukherjee, A., Agrawal, M., Park, R. J., Oak, Y. J., and Yue, X.: Ozone pollution threatens the
566 production of major staple crops in East Asia, *Nat. Food*, 3, 47-+, 10.1038/s43016-021-00422-6,
567 2022.
- 568 Gopikrishnan, G. S. and Kuttippurath, J.: Global tropical and extra-tropical tropospheric ozone trends
569 and radiative forcing deduced from satellite and ozonesonde measurements for the period 2005–
570 2020. *Environ. Pollut.*, 361, 124869, 10.1016/j.envpol.2024.124869, 2024.
- 571 Gu, Y. X., Li, K., Xu, J. M., Liao, H., and Zhou, G. Q.: Observed dependence of surface ozone on
572 increasing temperature in Shanghai, China, *Atmos. Environ.*, 221,
573 10.1016/j.atmosenv.2019.117108, 2020.
- 574 Jiang, Z. J., Li, J., Lu, X., Gong, C., Zhang, L., and Liao, H.: Impact of western Pacific subtropical
575 high on ozone pollution over eastern China, *Atmos. Chem. Phys.*, 21, 2601-2613, 10.5194/acp-21-



- 576 2601-2021, 2021.
- 577 Kawano, N., Nagashima, T., and Sugata, S.: Changes in seasonal cycle of surface ozone over Japan
578 during 1980-2015, *Atmos. Environ.*, 279, 10.1016/j.atmosenv.2022.119108, 2022.
- 579 Kim, S. W., Kim, K. M., Jeong, Y., Seo, S., Park, Y., and Kim, J.: Changes in surface ozone in South
580 Korea on diurnal to decadal timescales for the period of 2001-2021, *Atmos. Chem. Phys.*, 23,
581 12867-12886, 10.5194/acp-23-12867-2023, 2023.
- 582 Lee, H. J., Chang, L. S., Jaffe, D. A., Bak, J., Liu, X., Abad, G. G., Jo, H. Y., Jo, Y. J., Lee, J. B., and
583 Kim, C. H.: Ozone Continues to Increase in East Asia Despite Decreasing NO₂:
584 Causes and Abatements, *Remote Sens.*, 13, 10.3390/rs13112177, 2021.
- 585 Lee, H. M. and Park, R. J.: Factors determining the seasonal variation of ozone air quality in South
586 Korea: Regional background versus domestic emission contributions, *Environ. Pollut.*, 308,
587 10.1016/j.envpol.2022.119645, 2022.
- 588 Li, F., Zheng, Q. P., Jiang, Y. C., Xun, A. P., Zhang, J. R., Zheng, H., and Wang, H.: Impact analysis of
589 super Typhoon 2114 'Chanthu' on the air quality of coastal cities in southeast China based on multi-
590 source measurements, *Atmosphere*, 14, 10.3390/atmos14020380, 2023a.
- 591 Li, K., Jacob, D. J., Liao, H., Shen, L., Zhang, Q., and Bates, K. H.: Anthropogenic drivers of 2013-
592 2017 trends in summer surface ozone in China, *Proc. Nat. Acad. Sci.*, 116, 422-427,
593 10.1073/pnas.1812168116, 2019.
- 594 Li, K., Jacob, D. J., Shen, L., Lu, X., De Smedt, I., and Liao, H.: Increases in surface ozone pollution
595 in China from 2013 to 2019: anthropogenic and meteorological influences, *Atmos. Chem. Phys.*,
596 20, 11423-11433, 10.5194/acp-20-11423-2020, 2020.
- 597 Li, K., Jacob, D. J., Liao, H., Qiu, Y. L., Shen, L., Zhai, S. X., Bates, K. H., Sulprizio, M. P., Song, S.
598 J., Lu, X., Zhang, Q., Zheng, B., Zhang, Y. L., Zhang, J. Q., Lee, H. C., and Kuk, S. K.: Ozone
599 pollution in the North China Plain spreading into the late-winter haze season, *Proc. Nat. Acad. Sci.*,
600 118, 10.1073/pnas.2015797118, 2021.
- 601 Li, M., Kurokawa, J., Zhang, Q., Woo, J. H., Morikawa, T., Chatani, S., Lu, Z., Song, Y., Geng, G.,
602 Hu, H., Kim, J., Cooper, O. R., and McDonald, B. C.: MIXv2: a long-term mosaic emission
603 inventory for Asia (2010–2017), *Atmos. Chem. Phys.*, 24, 3925-3952, 10.5194/acp-24-3925-2024,
604 2024.
- 605 Li, S., Yang, Y., Wang, H. L., Li, P. W., Li, K., Ren, L. L., Wang, P. Y., Li, B. J., Mao, Y. H., and Liao,
606 H.: Rapid increase in tropospheric ozone over Southeast Asia attributed to changes in precursor
607 emission source regions and sectors, *Atmos. Environ.*, 304, 10.1016/j.atmosenv.2023.119776,
608 2023b.
- 609 Liao, Z. H., Ling, Z. H., Gao, M., Sun, J. R., Zhao, W., Ma, P. K., Quan, J. N., and Fan, S. J.:
610 Tropospheric Ozone Variability Over Hong Kong Based on Recent 20 years (2000-2019)
611 Ozone-sonde Observation, *J. Geophys. Res. Atmos.*, 126, 10.1029/2020jd033054, 2021.
- 612 Lu, X., Zhang, L., Wang, X. L., Gao, M., Li, K., Zhang, Y. Z., Yue, X., and Zhang, Y. H.: Rapid
613 Increases in Warm-Season Surface Ozone and Resulting Health Impact in China Since 2013,
614 *Environ. Sci. Tech. Lett.*, 7, 240-247, 10.1021/acs.estlett.0c00171, 2020.
- 615 Lu, X., Hong, J. Y., Zhang, L., Cooper, O. R., Schultz, M. G., Xu, X. B., Wang, T., Gao, M., Zhao, Y.
616 H., and Zhang, Y. H.: Severe Surface Ozone Pollution in China: A Global Perspective, *Environ.*
617 *Sci. Tech. Lett.*, 5, 487-494, 10.1021/acs.estlett.8b00366, 2018.
- 618 Lu, X., Liu, Y., Su, J., Weng, X., Ansari, T., Zhang, Y., He, G., Zhu, Y., Wang, H., Zeng, G., Li, J., He,
619 C., Li, S., Amnuaylojaroen, T., Butler, T., Fan, Q., Fan, S., Forster, G. L., Gao, M., Hu, J., Kanaya,
620 Y., Latif, M. T., Lu, K., Nédélec, P., Nowack, P., Sauvage, B., Xu, X., Zhang, L., Li, K., Koo, J.-



- 621 H., and Nagashima, T.: Tropospheric ozone trends and attributions over East and Southeast Asia in
622 1995–2019: An integrated assessment using statistical methods, machine learning models, and
623 multiple chemical transport models, *EGUsphere*, 10.5194/egusphere-2024-3702, 2024.
- 624 Lyu, X., Li, K., Guo, H., Morawska, L., Zhou, B. N., Zeren, Y., Jiang, F., Chen, C. H., Goldstein, A.
625 H., Xu, X. B., Wang, T., Lu, X., Zhu, T., Querol, X., Chatani, S., Latif, M. T., Schuch, D., Sinha,
626 V., Kumar, P., Mullins, B., Seguel, R., Shao, M., Xue, L. K., Wang, N., Chen, J. M., Gao, J., Chai,
627 F. H., Simpson, I., Sinha, B., and Blake, D. R.: A synergistic ozone-climate control to address
628 emerging ozone pollution challenges, *One Earth*, 6, 964-977, 10.1016/j.oneear.2023.07.004, 2023.
- 629 Ma, Z., Xu, J., Quan, W., Zhang, Z., Lin, W., and Xu, X.: Significant increase of surface ozone at a
630 rural site, north of eastern China. *Atmos. Chem. Phys.*, 16(6), 3969-3977, 2016.
- 631 Nagashima, T., Sudo, K., Akimoto, H., Kurokawa, J., and Ohara, T.: Long-term change in the source
632 contribution to surface ozone over Japan, *Atmos. Chem. Phys.*, 17, 8231-8246, 10.5194/acp-17-
633 8231-2017, 2017.
- 634 Neu, J. L., Flury, T., Manney, G. L., Santee, M. L., Livesey, N. J., and Worden, J.: Tropospheric ozone
635 variations governed by changes in stratospheric circulation. *Nat. Geosci.*, 7(5), 340-344, 2014.
- 636 Park, S. S., Kim, J., Cho, H. K., Lee, H., Lee, Y., and Miyagawa, K.: Sudden increase in the total ozone
637 density due to secondary ozone peaks and its effect on total ozone trends over Korea, *Atmos.*
638 *Environ.*, 47, 226-235, 10.1016/j.atmosenv.2011.11.011, 2012.
- 639 Salvador, C. M. G., Alindajao, A. D., Burdeos, K. B., Lavapie, M. A. M., Yee, J. R., Bautista, A. T.,
640 Pabroa, P. C. B., and Capangpangan, R. Y.: Assessment of Impact of Meteorology and Precursor
641 in Long-term Trends of PM and Ozone in a Tropical City, *Aerosol Air Qual. Res.*, 22,
642 10.4209/aaqr.210269, 2022.
- 643 Sukkhum, S., Lim, A., Ingviya, T., and Saelim, R.: Seasonal Patterns and Trends of Air Pollution in
644 the Upper Northern Thailand from 2004 to 2018, *Aerosol Air Qual. Res.*, 22, 10.4209/aaqr.210318,
645 2022.
- 646 Sun, L., Xue, L., Wang, T., Gao, J., Ding, A., Cooper, O.R., Lin, M., Xu, P., Wang, Z., Wang, X. and
647 Wen, L.: Significant increase of summertime ozone at Mount Tai in Central Eastern China. *Atmos.*
648 *Chem. Phys.*, 16(16), 10637-10650, 2016.
- 649 Sun, H. Z., van Daalen, K. R., Morawska, L., Guillas, S., Giorio, C., Di, Q., Kan, H., Loo, E. X.-L.,
650 Shek, L. P., Watts, N., Guo, Y., and Archibald, A. T.: An estimate of global cardiovascular mortality
651 burden attributable to ambient ozone exposure reveals urban-rural environmental injustice, *One*
652 *Earth*, 7, 1803-1819, <https://doi.org/10.1016/j.oneear.2024.08.018>, 2024.
- 653 Vingarzan, R. (2004). A review of surface ozone background levels and trends. *Atmos. Environ.*,
654 38(21), 3431-3442, 2004.
- 655 Wang, H., Lu, X., Palmer, P. I., Zhang, L., Lu, K., Li, K., Nagashima, T., Koo, J.-H., Tanimoto, H.,
656 Wang, H., Gao, M., He, C., Wu, K., Fan, S., and Zhang, Y.: Deciphering decadal urban ozone trends
657 from historical records since 1980, *Natl. Sci. Rev.*, 11, 10.1093/nsr/nwae369, 2024.
- 658 Wang, H. L., Lu, X., Jacob, D. J., Cooper, O. R., Chang, K. L., Li, K., Gao, M., Liu, Y. M., Sheng, B.
659 S., Wu, K., Wu, T. W., Zhang, J., Sauvage, B., Nédélec, P., Blot, R., and Fan, S. J.: Global
660 tropospheric ozone trends, attributions, and radiative impacts in 1995-2017: an integrated analysis
661 using aircraft (IAGOS) observations, ozonesonde, and multi-decadal chemical model simulations,
662 *Atmos. Chem. Phys.*, 22, 13753-13782, 10.5194/acp-22-13753-2022, 2022b.
- 663 Wang, T., Dai, J. N., Lam, K. S., Nan Poon, C., and Brasseur, G. P.: Twenty-Five Years of Lower
664 Tropospheric Ozone Observations in Tropical East Asia: The Influence of Emissions and Weather
665 Patterns, *Geophys. Res. Lett.*, 46, 11463-11470, 10.1029/2019gl084459, 2019.



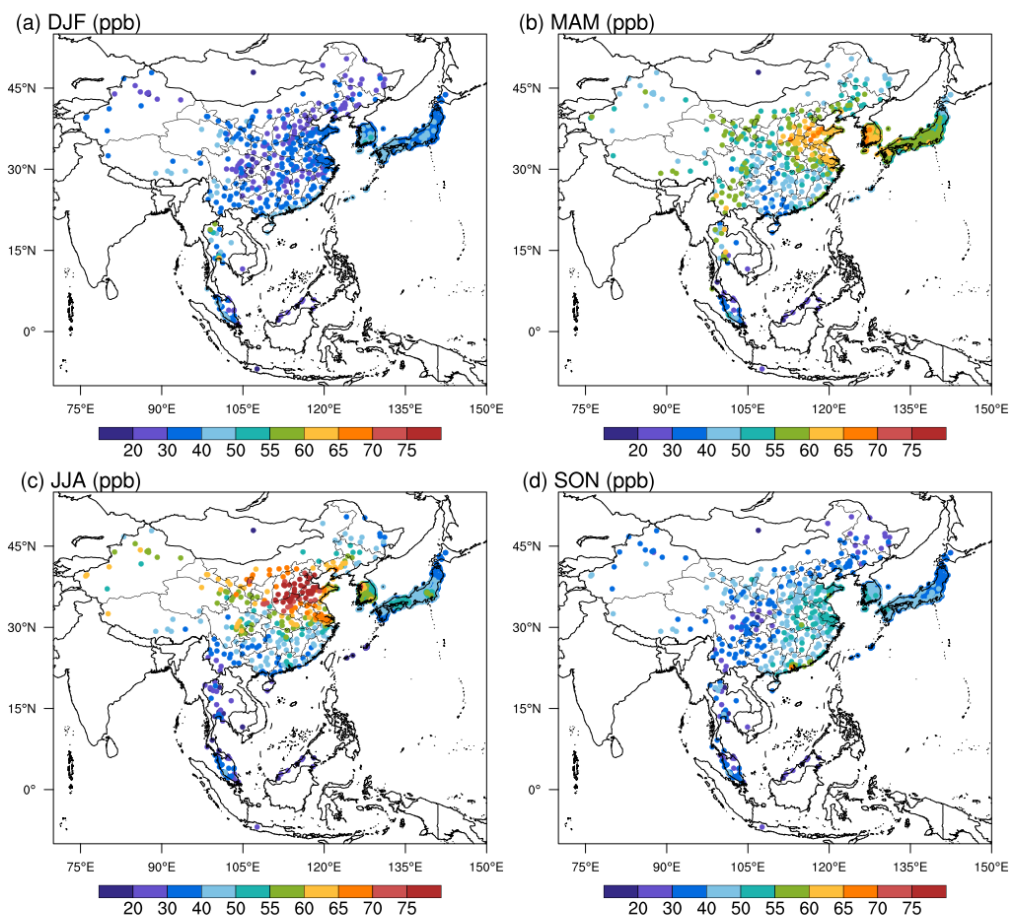
- 666 Wang, X. L., Fu, T. M., Zhang, L., Lu, X., Liu, X., Amnuaylojaroen, T., Latif, M. T., Ma, Y. P., Zhang,
667 L. J., Feng, X., Zhu, L., Shen, H. Z., and Yang, X.: Rapidly Changing Emissions Drove Substantial
668 Surface and Tropospheric Ozone Increases Over Southeast Asia, *Geophys. Res. Lett.*, 49,
669 10.1029/2022gl100223, 2022a.
- 670 Xu, X. B., Lin, W. L., Xu, W. Y., Jin, J. L., Wang, Y., Zhang, G., Zhang, X. C., Ma, Z. Q., Dong, Y. Z.,
671 Ma, Q. L., Yu, D. J., Li, Z., Wang, D. D., and Zhao, H. R.: Long-term changes of regional ozone
672 in China: implications for human health and ecosystem impacts, *Elementa*, 8,
673 10.1525/elementa.409, 2020.
- 674 Xue, L., Ding, A., Cooper, O., Huang, X., Wang, W., Zhou, D., Wu, Z., McClure-Begley, A.,
675 Petropavlovskikh, I., Andreae, M.O. and Fu, C.: ENSO and Southeast Asian biomass burning
676 modulate subtropical trans-Pacific ozone transport. *Natl. Sci. Rev.*, 8(6), nwaal32, 2021.
- 677 Ye, X. P., Zhang, L., Wang, X. L., Lu, X., Jiang, Z. J., Lu, N., Li, D. Y., and Xu, J. Y.: Spatial and
678 temporal variations of surface background ozone in China analyzed with the grid-stretching
679 capability of GEOS-Chem High Performance, *Sci. Total Environ.*, 914,
680 10.1016/j.scitotenv.2024.169909, 2024.
- 681 Yin, Z., Wang, H., Li, Y., Ma, X., and Zhang, X.: Links of climate variability in Arctic sea ice, Eurasian
682 teleconnection pattern and summer surface ozone pollution in North China. *Atmos. Chem. Phys.*,
683 19(6), 3857-3871, 2019.
- 684 Yuan, S., Stuart, A.M., Laborte, A.G., Rattalino Edreira, J.I., Dobermann, A., Kien, L.V.N., Thúy, L.T.,
685 Paotrong, K., Traesang, P., Tint, K.M. and San, S.S.: Southeast Asia must narrow down the yield
686 gap to continue to be a major rice bowl. *Nat. Food*, 3(3), 217-226, 2022.
- 687 Zanis, P., Akritidis, D., Turnock, S., Naik, V., Szopa, S., Georgoulas, A.K., Bauer, S.E., Deushi, M.,
688 Horowitz, L.W., Keeble, J. and Le Sager, P.: Climate change penalty and benefit on surface ozone:
689 a global perspective based on CMIP6 earth system models. *Environ. Res. Lett.*, 17(2), 024014,
690 2022.
- 691 Zeng, Y. S., Zhang, J. Q., Li, D., Liao, Z. H., Bian, J. C., Bai, Z. X., Shi, H. R., Xuan, Y. J., Yao, Z. D.,
692 and Chen, H. B.: Vertical distribution of tropospheric ozone and its sources of precursors over
693 Beijing: Results from ~ 20 years of ozonesonde measurements based on clustering analysis, *Atmos.*
694 *Res.*, 284, 10.1016/j.atmosres.2023.106610, 2023.
- 695 Zhan, C. C. and Xie, M.: Exploring the link between ozone pollution and stratospheric intrusion under
696 the influence of tropical cyclone Ampil, *Sci. Total Environ.*, 828, 10.1016/j.scitotenv.2022.154261,
697 2022.
- 698 Zhang, J., Li, D., Bian, J., Xuan, Y., Chen, H., Bai, Z., Wan, X., Zheng, X., Xia, X. and Lü, D.: Long-
699 term ozone variability in the vertical structure and integrated column over the North China Plain:
700 results based on ozonesonde and Dobson measurements during 2001–2019. *Environ. Res. Lett.*,
701 16(7), 074053, 2021.
- 702 Zhang, X. Y., Xu, W. Y., Zhang, G., Lin, W. L., Zhao, H. R., Ren, S. X., Zhou, G. S., Chen, J. M., and
703 Xu, X. B.: First long-term surface ozone variations at an agricultural site in the North China Plain:
704 Evolution under changing meteorology and emissions, *Sci. Total Environ.*, 860,
705 10.1016/j.scitotenv.2022.160520, 2023.
- 706 Zhang, Y. N., Xiang, Y. R., Chan, L. Y., Chan, C. Y., Sang, X. F., Wang, R., and Fu, H. X.: Procuring
707 the regional urbanization and industrialization effect on ozone pollution in Pearl River Delta of
708 Guangdong, China. *Atmos. Environ.*, 45(28), 4898-4906, 2011.
- 709 Zhao, Z. J. and Wang, Y. X.: Influence of the West Pacific subtropical high on surface ozone daily
710 variability in summertime over eastern China, *Atmos. Environ.*, 170, 197-204,



711 10.1016/j.atmosenv.2017.09.024, 2017.
712 Zheng, B., Tong, D., Li, M., Liu, F., Hong, C., Geng, G., Li, H., Li, X., Peng, L., Qi, J., Yan, L., Zhang,
713 Y., Zhao, H., Zheng, Y., He, K., and Zhang, Q.: Trends in China's anthropogenic emissions since
714 2010 as the consequence of clean air actions, *Atmos. Chem. Phys.*, 18, 14095–14111,
715 <https://doi.org/10.5194/acp-18-14095-2018>, 2018.
716 Zhou, Y., Yang, Y., Wang, H., Wang, J., Li, M., Li, H., Wang, P., Zhu, J., Li, K. and Liao, H.: Summer
717 ozone pollution in China affected by the intensity of Asian monsoon systems. *Sci. Total Environ.*,
718 849, 157785, 2022.
719
720
721
722
723
724
725
726
727
728
729
730
731
732
733
734
735
736
737
738
739



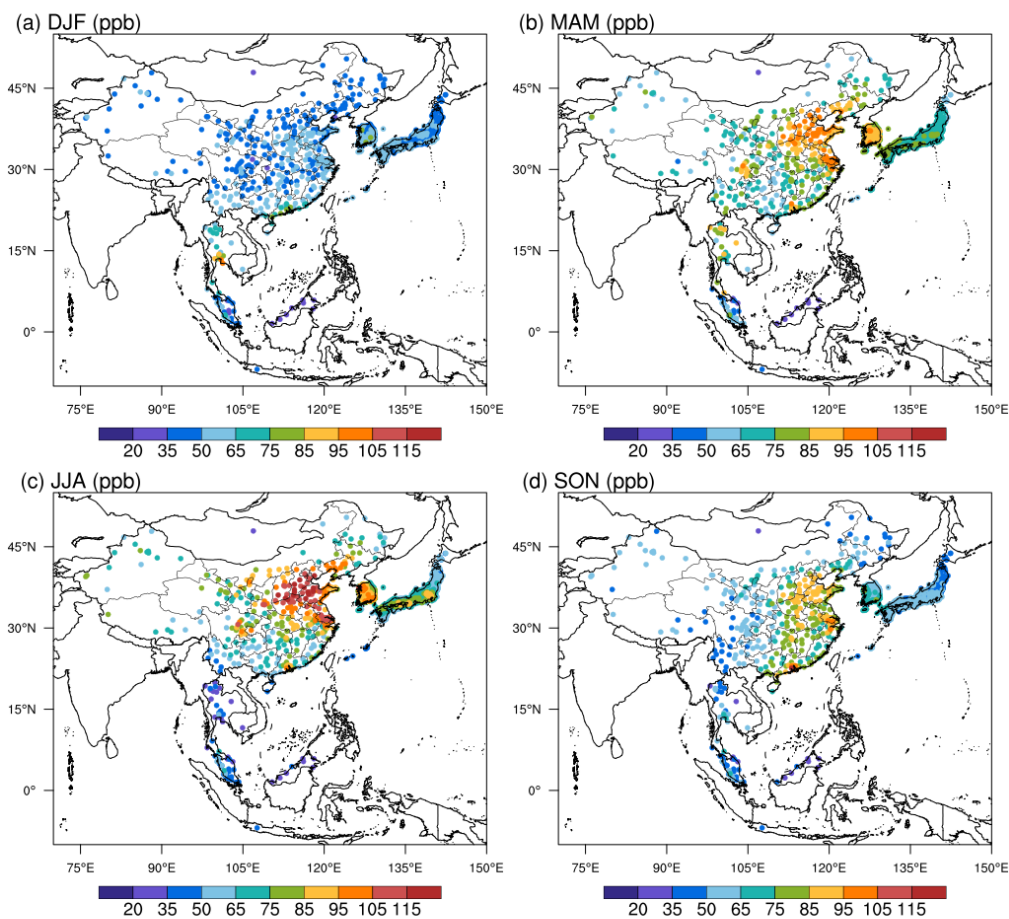
740 **Figures**



741

742 **Figure 1.** The observed seasonal mean MDA8 ozone (ppb) in (a) DJF, (b) MAM, (c) JJA, and (d) SON
743 averaged during 2017-2021 over East Asia and Southeast Asia. There are eight countries with surface
744 ozone measurements, including Cambodia (1 site), China (360 sites), Indonesia (1 site), Japan (1187
745 sites), Malaysia (66 sites), Mongolia (1 site), South Korea (473 sites), and Thailand (25 sites).

746



747

748 **Figure 2.** Same as Figure 1 but for the seasonal 95th percentile MDA8 ozone (ppb) averaged over
749 2017-2021. This metric represents the extreme high ozone values that are related to short-term ozone
750 exposure.

751

752

753

754

755

756

757

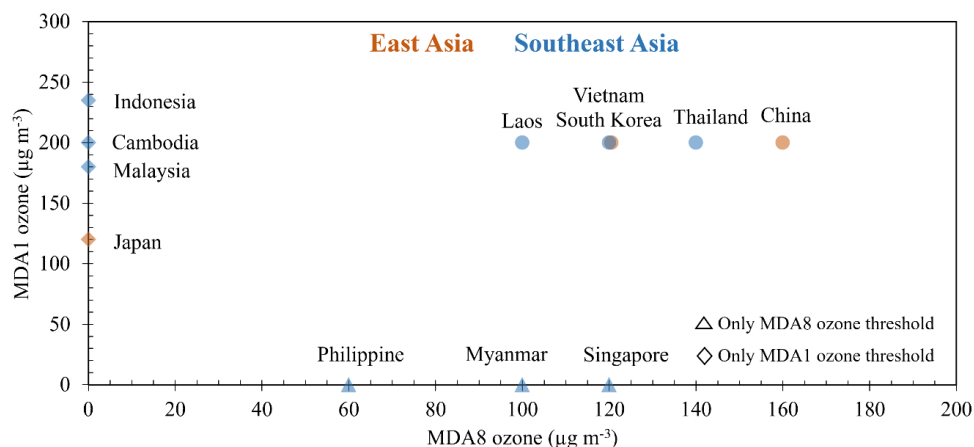
758

759

760

761

762



763

764 **Figure 3.** The national ambient ozone air quality standard in East Asia and Southeast Asia. The
765 maximum daily 8 h average (MDA8) and/or maximum daily 1 h average (MDA1) ozone thresholds
766 are routinely adopted but they vary greatly in different countries. The sources for these thresholds
767 are given in Table S1. Under standard conditions (1013 hPa, 273 K), 1 ppb = 2.14 µg m⁻³.

768

769

770

771

772

773

774

775

776

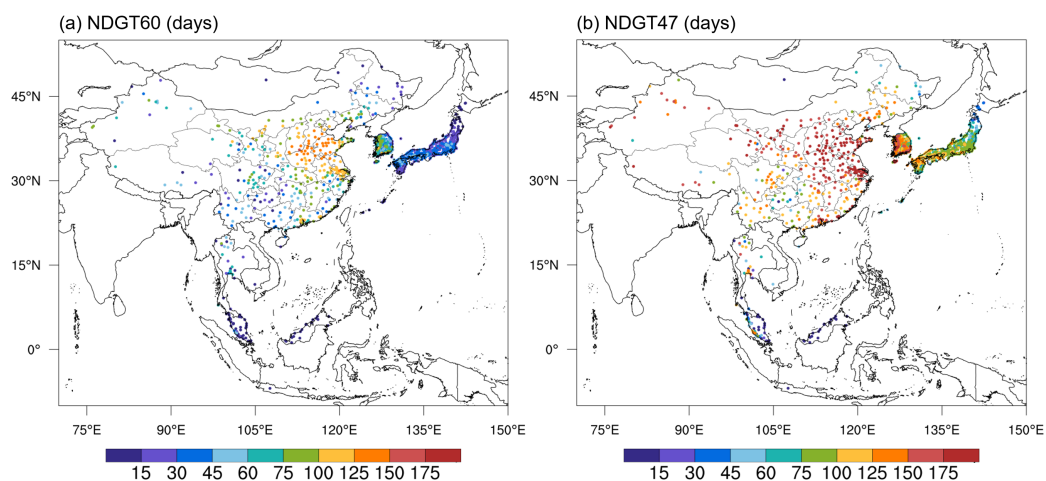
777

778

779

780

781



782

783 **Figure 4.** Annual number of days with daily MDA8 ozone greater than 60 ppb (NDGT60) and greater
784 than the WHO standard of $100 \mu\text{g m}^{-3}$ (NDGT47) averaged over 2017-2021. Under standard conditions
785 (1013 hPa, 273 K), $1 \text{ ppb} = 2.14 \mu\text{g m}^{-3}$.

786

787

788

789

790

791

792

793

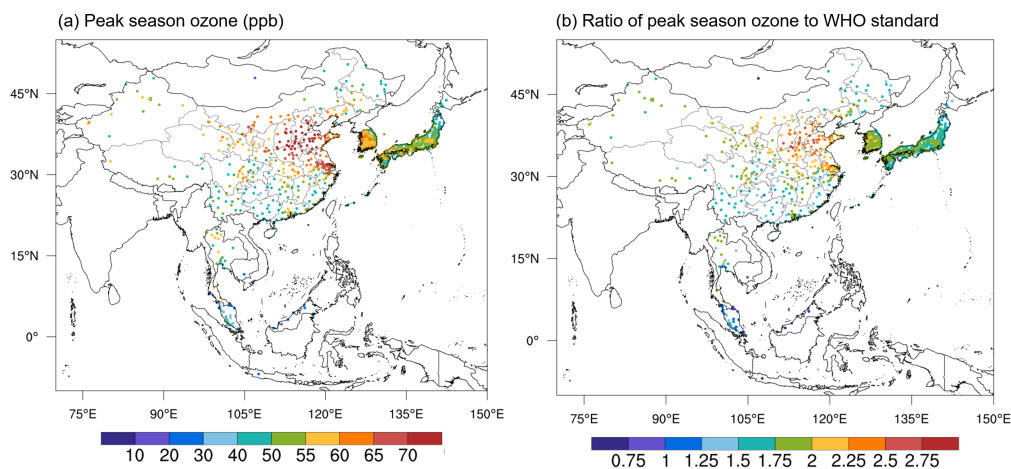
794

795

796

797

798



799

800 **Figure 5.** Annual mean peak season ozone (ppb) averaged over 2017-2021 (a) and the ratio of the
801 observed peak season ozone to the WHO standard of 60 $\mu\text{g m}^{-3}$ (b). As introduced by the WHO, the
802 concentration of peak season ozone is calculated by using the average monthly MDA8 ozone
803 concentration in the six consecutive months with the highest six-month running-average ozone
804 concentration. This new metric represents the long-term ozone exposure.

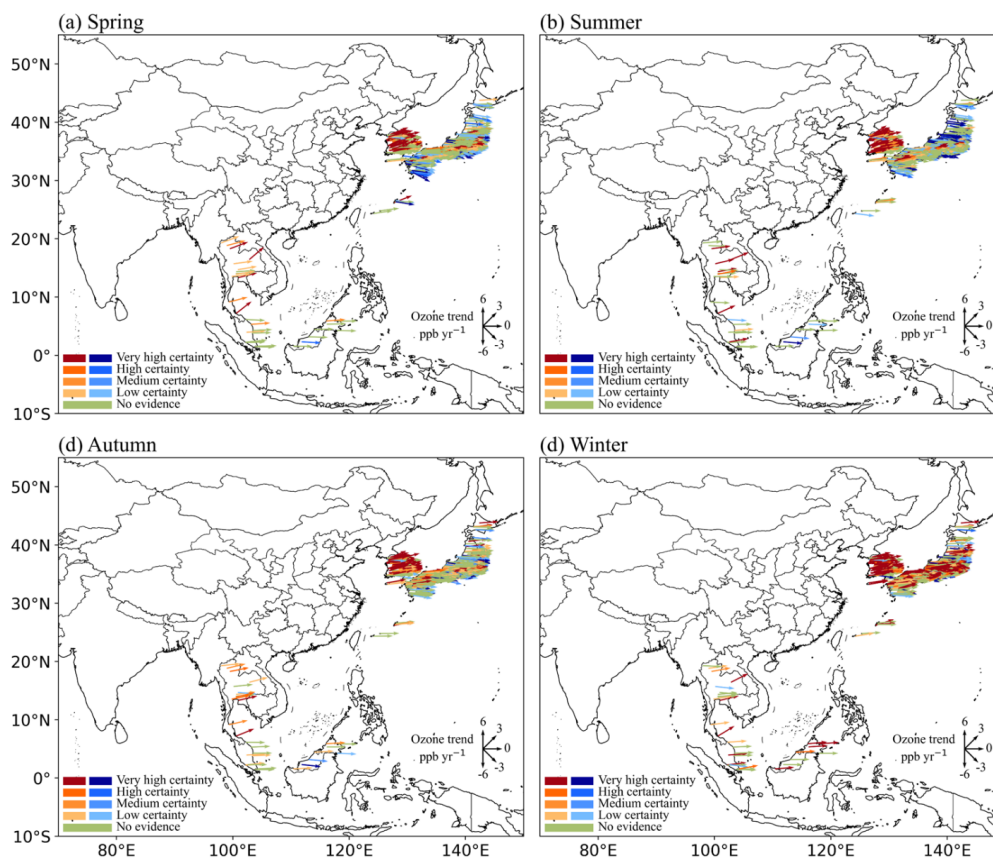
805

806

807

808

809



810

811 **Figure 6.** The observed 2005-2021 ozone trends (ppb yr⁻¹) during (a) spring, (b) summer, (c) autumn,
 812 and (d) winter over East Asia and Southeast Asia. Here it only includes ozone measurements from
 813 Malaysia (19 sites), Japan (946 sites), South Korea (226 sites), and Thailand (13 sites). National
 814 surface ozone data in China is not available before 2013, therefore not shown in this figure. To follow
 815 the trend reliability scale recommended by the TOAR II, here we use “very high certainty” to denote
 816 $p \leq 0.01$, “high certainty” to denote $0.05 \geq p > 0.01$, and “medium certainty” to denote $0.10 \geq p > 0.05$;
 817 positive trends are in red and negative trends are in blue.

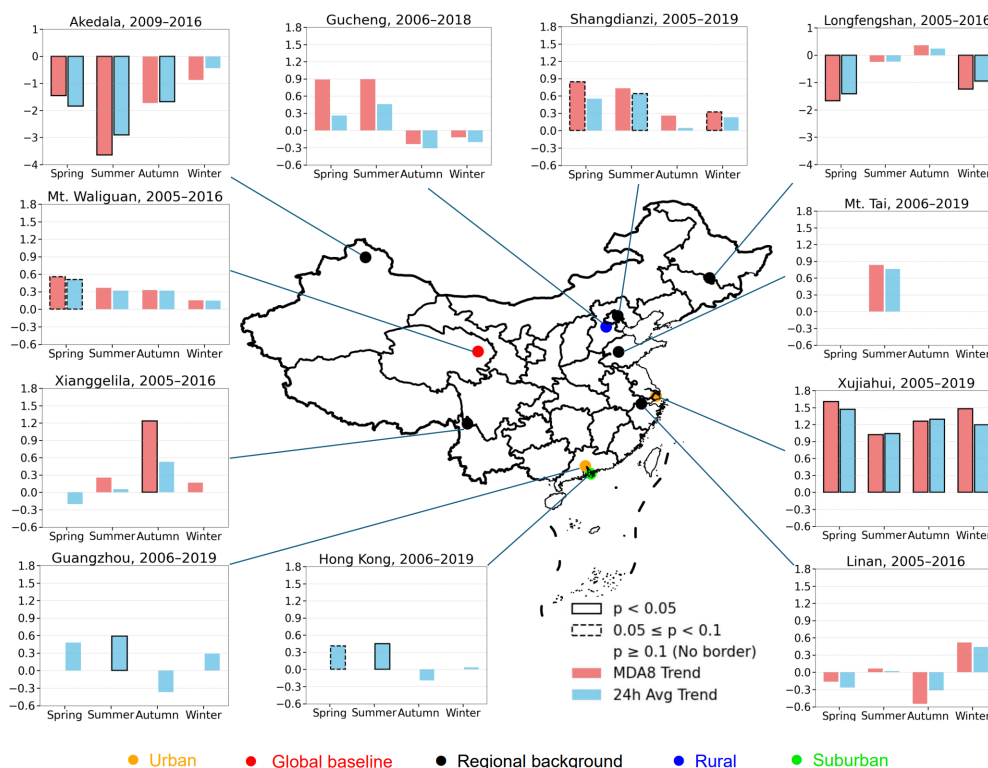
818

819

820

821

822



823

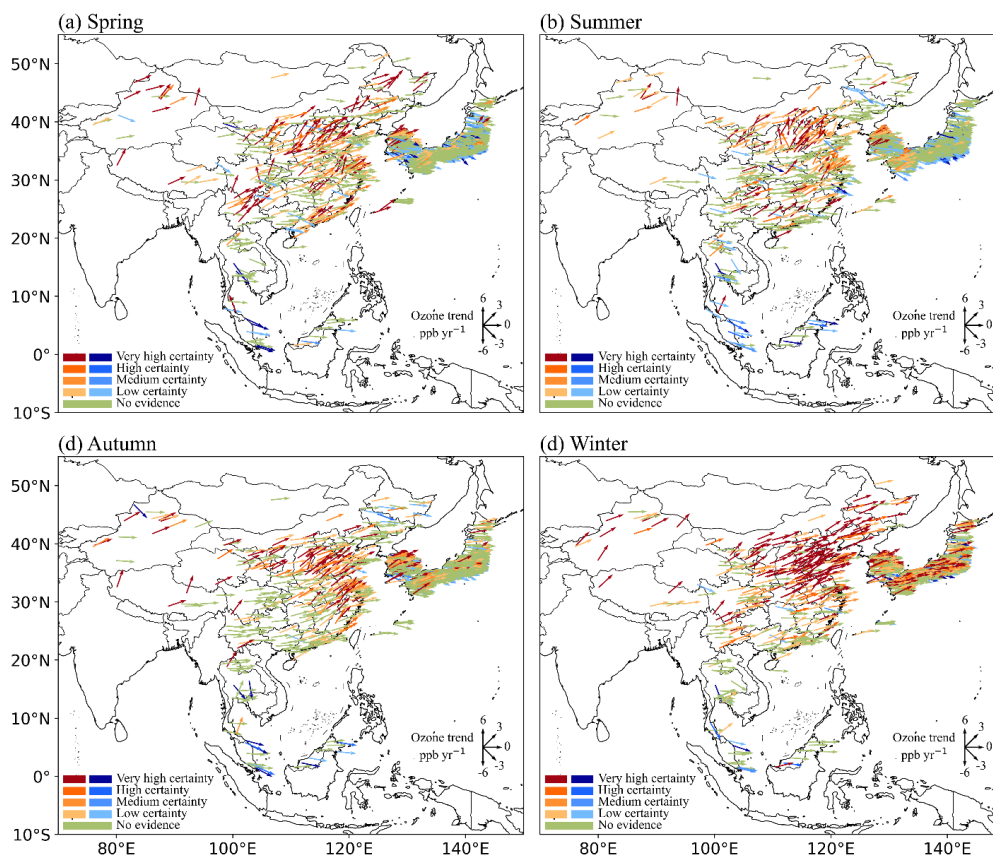
824 **Figure 7.** The observed long-term ozone trends after 2005 in 11 measurement sites over China. There
 825 are 1 global baseline station, 5 regional background stations, 1 rural station, 1 suburban station, and 2
 826 urban stations. Due to data availability, we use the MDA8 ozone and/or 24-hour mean ozone in the
 827 calculation of ozone trends. The p -value for estimated ozone trends is also highlighted by rectangles.

828

829

830

831



832

833 **Figure 8.** Same with Figure 6 but for the observed 2013-2021 ozone trends (ppb yr⁻¹) over East Asia
 834 and Southeast Asia. Here it includes ozone measurements from China (335 sites), Malaysia (19 sites),
 835 Mongolia (1 site), Japan (1130 sites), South Korea (270 sites), and Thailand (22 sites). To follow the
 836 trend reliability scale recommended by the TOAR II, here we use “very high certainty” to denote $p \leq$
 837 0.01, “high certainty” to denote $0.05 \geq p > 0.01$, and “medium certainty” to denote $0.10 \geq p > 0.05$;
 838 positive trends are in red and negative trends are in blue.

839

840

841

842

843

844

845

846

847

848

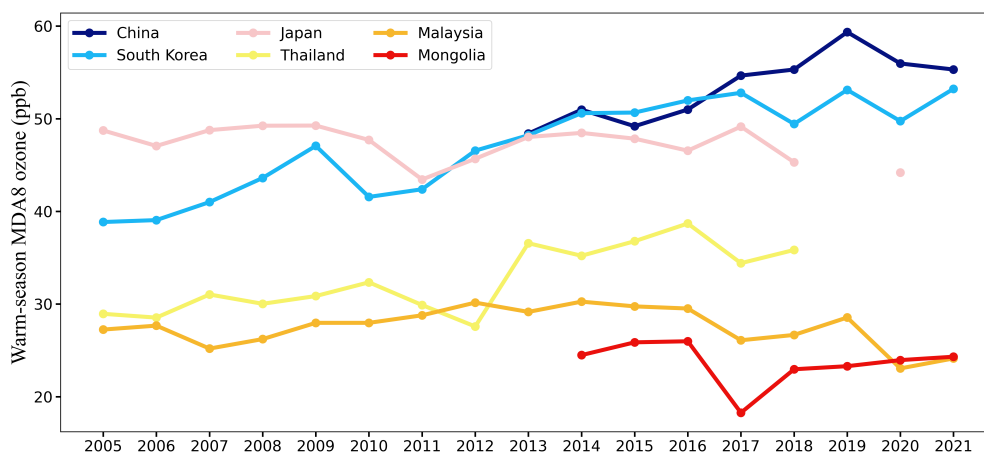
849

850

851



852



853

854 **Figure 9.** The observed national mean MDA8 ozone (ppb) during warm seasons (April to September)
855 from 2005 to 2021 in East Asia and Southeast Asia.

856

857

858

859

860

861

862

863

864

865

866

867

868

869

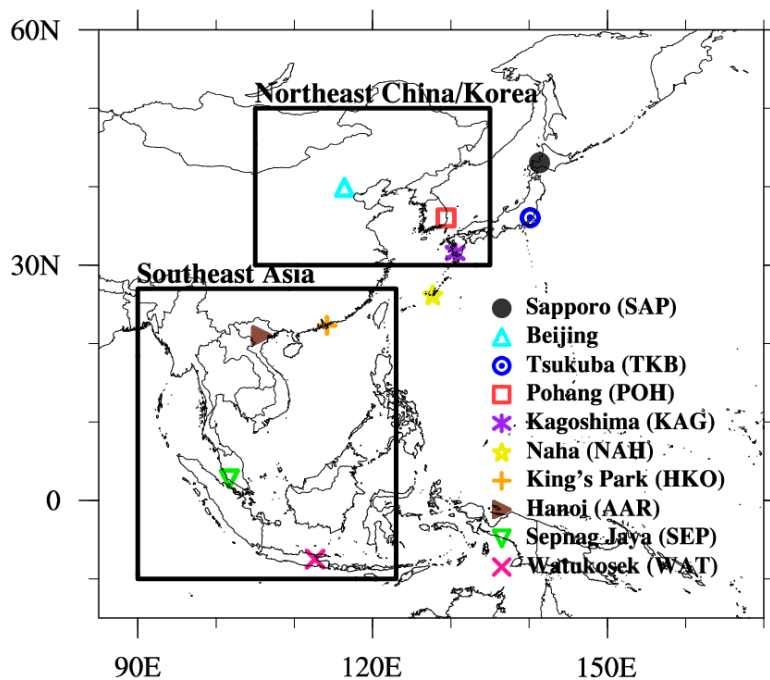
870

871

872

873

874



875

876 **Figure 10.** Map showing the location of ozonesonde sites and the coverage of the IAGOS
877 measurements considered in this study.

878

879

880

881

882

883

884

885

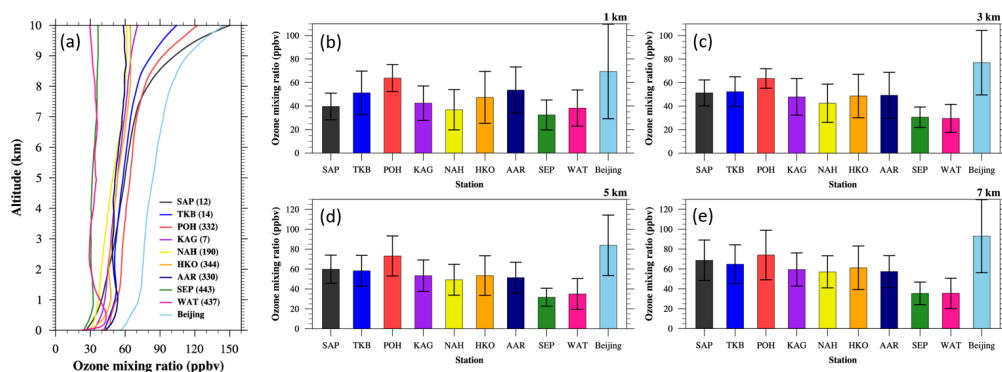
886

887

888

889

890



891

892

893 **Figure 11.** (a) Climatological mean vertical ozone profiles of 10 ozonesonde sites in the troposphere
894 (from 0 to 10 km altitude) are compared. Also, mean ozone mixing ratio values of 10 ozonesonde sites
895 at (b) 1 km, (c) 3 km, (d) 5 km, and (e) 7 km altitude are compared. Error-bar shows the 1-sigma
896 standard deviation range.

897

898

899

900

901

902

903

904

905

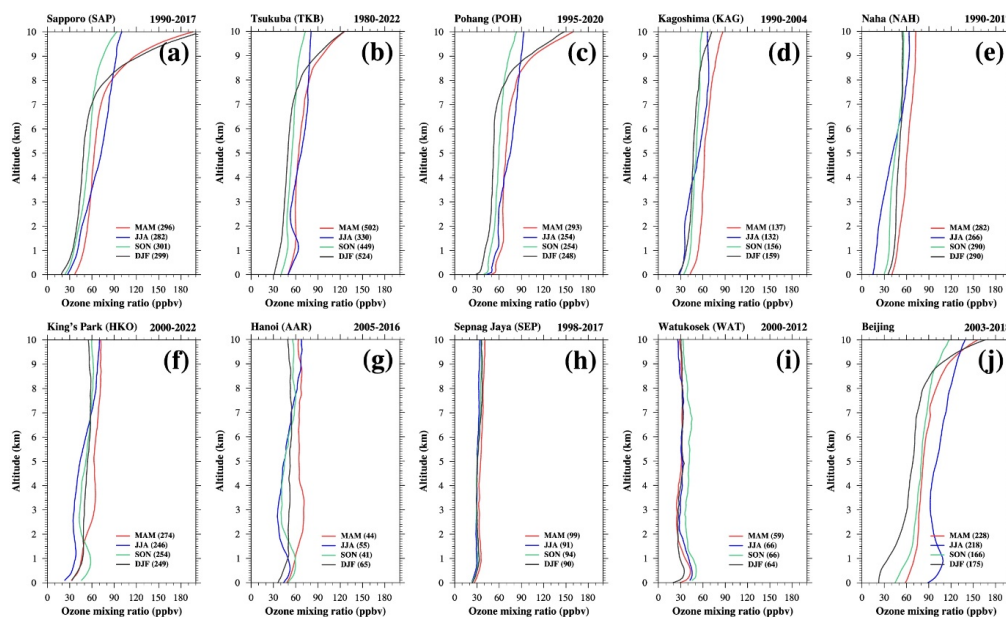
906

907

908

909

910



911

912

913 **Figure 12.** Seasonal mean vertical ozone profiles at (a) Sapporo (SAP), (b) Tsukuba (TKB), (c) Pohang
 914 (POH), (d) Kagoshima (KAG), (e) Naha (NAH), (f) King's park (HKO), (g) Hanoi (AAR), (h) Sepang
 915 Jaya (SEP), (i) Watukosek, and (j) Beijing site: March-April-May (MAM, red), June-July-August (JJA,
 916 blue), September-October-November (SON, green), and December-January-February (DJF).

917

918

919

920

921

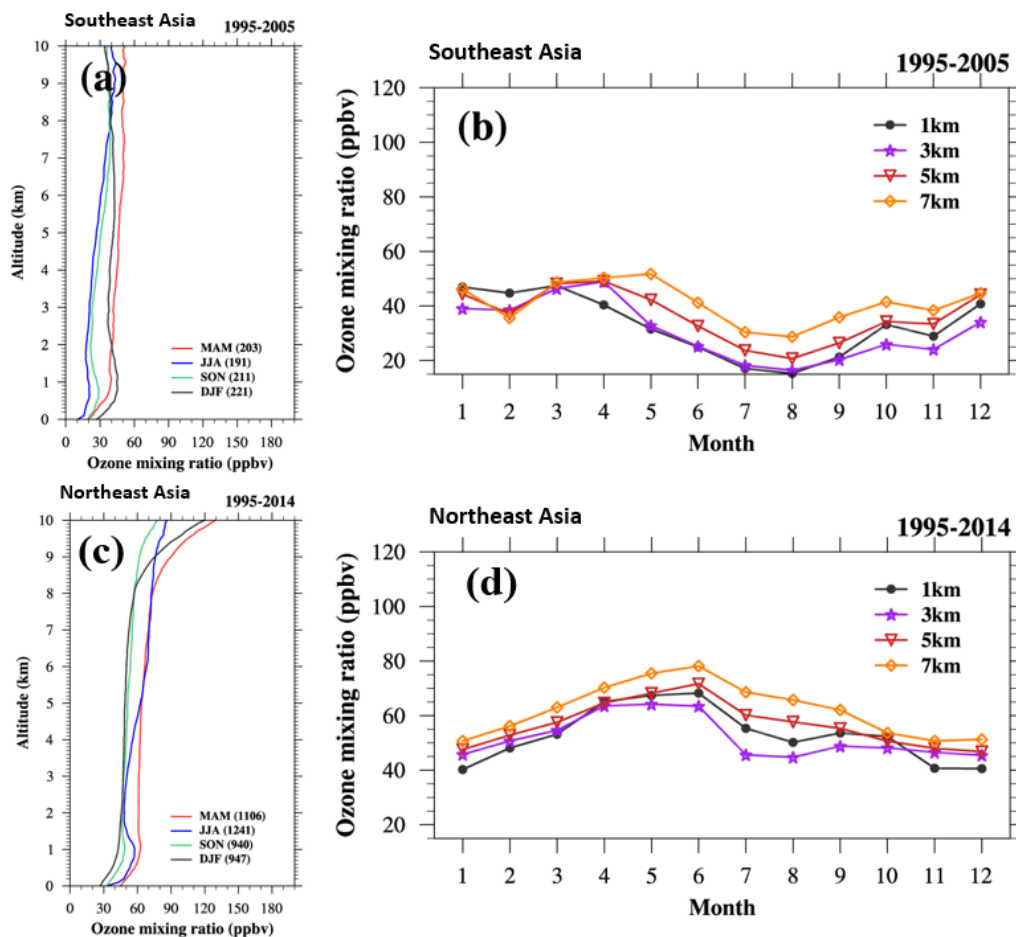
922

923

924

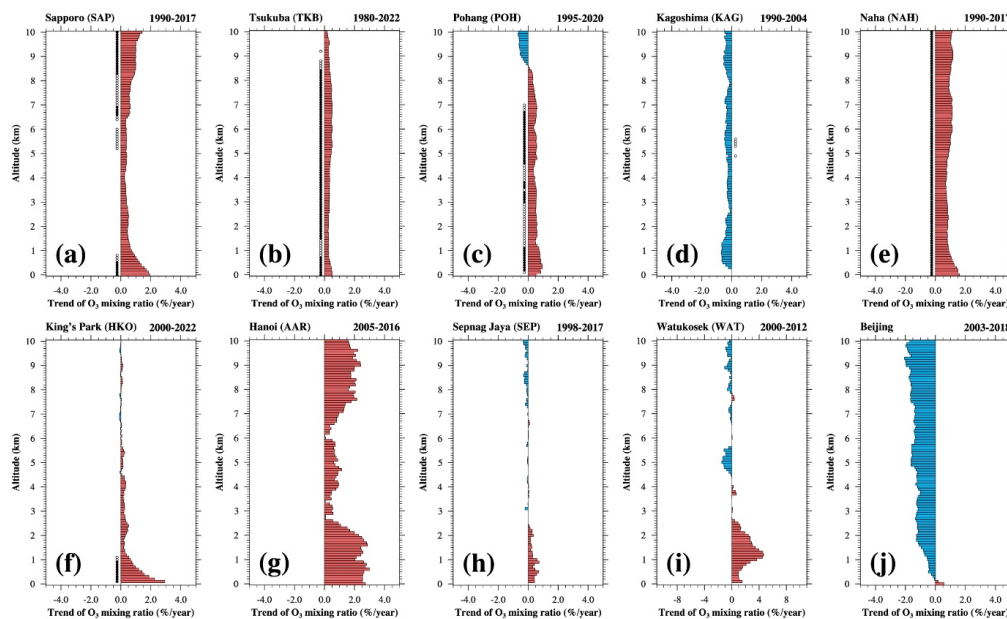
925

926



927
928
929
930
931
932
933
934
935
936
937
938

Figure 13. Analysis of the IAGOS measurements: (a) Seasonal mean vertical ozone profiles in Southeast Asia during March-April-May (MAM, red), June-July-August (JJA, blue), September-October-November (SON, green), and December-January-February (DJF, black), (b) monthly mean ozone variation of 1-km (black), 3-km (purple), 5-km (red), and 7-km (orange) altitudes in Southeast Asia, (c) seasonal mean vertical ozone profiles in Northeast Asia during MAM (red), JJA (blue), SON (green), and DJF (black), and (d) Monthly mean ozone variation of 1-km (black), 3-km (purple), 5-km (red), and 7-km (orange) altitudes in Northeast Asia.



939

940

941 **Figure 14.** Long-term trends of annual mean ozone per 100-m range from 0 to 10 km altitude at (a)
 942 Sapporo (SAP), (b) Tsukuba (TKB), (c) Pohang (POH), (d) Kagoshima (KAG), (e) Naha (NAH), (f)
 943 King's park (HKO), (g) Hanoi (AAR), (h) Sepang Jaya (SEP), (i) Watukosek, and (j) Beijing site.
 944 Orange color means increasing, and blue color means decreasing trend. Black dot indicates that the
 945 trend is statistically significant having a p -value smaller than 0.01, and white dot does that the trend is
 946 statistically significant having a p -value between 0.01 and 0.05.

947

948

949

950

951

952

953

954

955

956

957

958

959

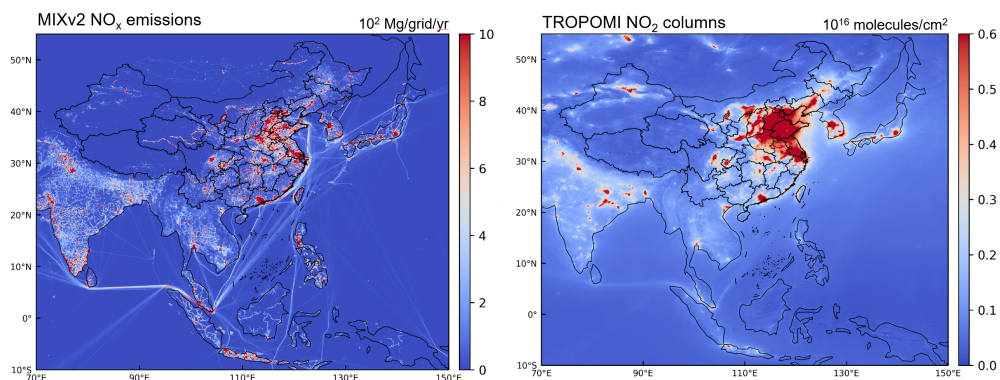
960

961

962

963

964

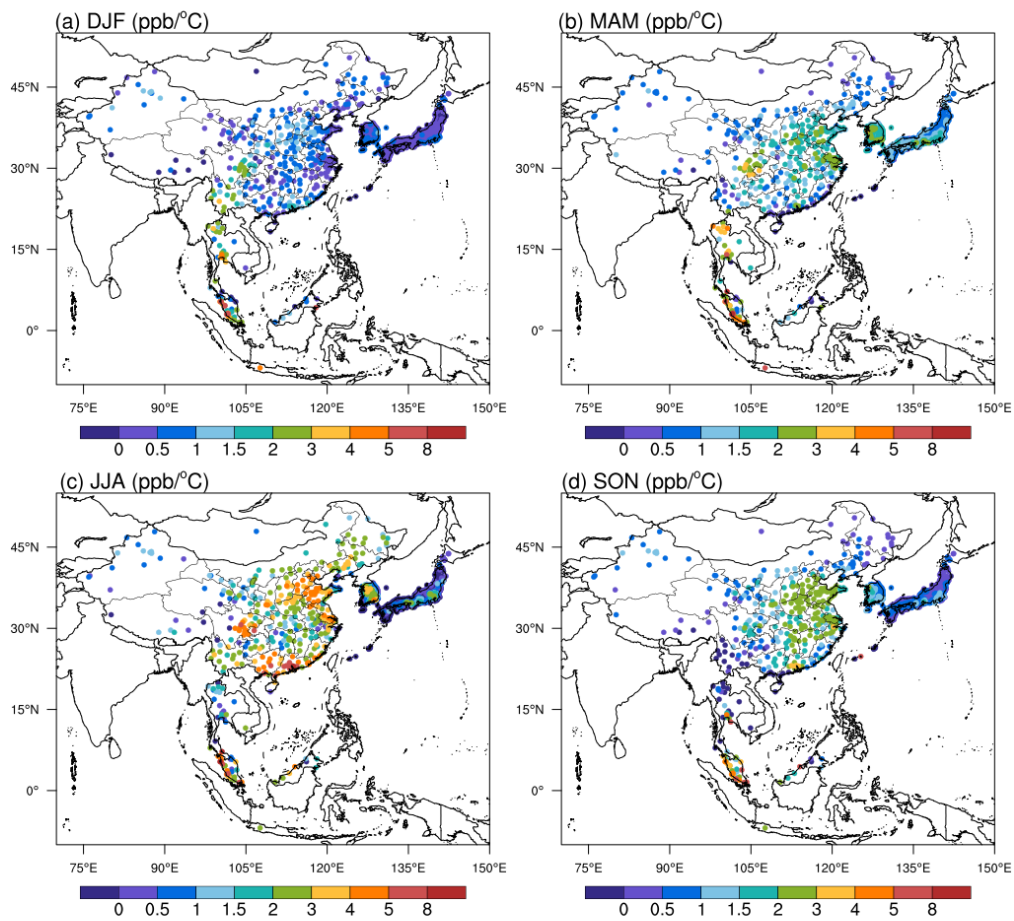


965

966 **Figure 15.** The spatial distribution of bottom-up NO_x emissions from MIXv2 inventory (left) and the
967 TROPOMI satellite derived NO₂ columns (right). Due to the data availability, emission data for year
968 2017 and satellite data for year 2019 are used to represent the present-day level (2017-2021),
969 respectively.

970

971



972

973 **Figure 16.** The observed 50th percentile regression slope (ppb °C⁻¹) between daily surface MDA8
974 ozone and daily maximum 2-m air temperature in (a) DJF, (b) MAM, (c) JJA, and (d) SON averaged
975 over 2017-2021.